BULLETIN OF THE POLISH ACADEMY OF SCIENCES
TECHNICAL SCIENCES, Vol. 61, No. 4, 2013
DOI: 10.2478/bpasts-2013-0103

The dynamics of the human arm with an observer for the capture of body motion parameters

A. BABIARZ* , R. BIEDA, K. JASKOT, and J. KLAMKA

Institute of Automatic Control, Silesian University of Technology, 16 Akademicka St., 44-101 Gliwice, Poland

Abstract. The paper presents an analysis of a mathematical model of the human arm dynamics in terms of observability. The purpose of the performed experiments is the selection of an observer for the possibility of arm tracking. The arm model is based on the two-link manipulator moving horizontally and vertically. For the study a model was linearized and the model part responsible for the work of human muscles was omitted. The experimental part involved simulated measurements of the motion parameters that imitate real-IMU (Inertial Measurement Unit) measurements. Finally, the simulation results using the observer in the form of a Kalman filter and the particle filter have been presented.

Key words: human arm, observability, Kalman filter, particle filter.

1. Introduction

The realistic construction of human body is very important in terms of medical applications, as well as entertainment. A very important aspect of the research is to understand the rules of the complex motion of kinematic links occurring during the movement of any part of our body. In the literature we can find some ways that represent human motion. Some of them are based on biomechanical information along with a very accurate representation of the muscles operation [1, 2], and some apply only to the motion analysis without the dynamics of the body [3–5].

A very difficult problem is also the dynamics stability of the body in combination with complex upper limb movements [6–8]. To this end, there are attempts to represent kinematic actuators based on DC motors [6]. The complexity of dynamics description of even a simple human movement determines the repeatability and accuracy of movement. It is very important in terms of application of appropriate constructions in medicine and in rehabilitation devices.

Papers [9–11] have proposed a human motion control schemes and proposals of devices supporting motion in disabled people (mainly supporting the movement of the upper limbs). For medical purposes the EMG signals, which can mimic an actual signals of a healthy person, to reproduce body movements [12, 13] are also used.

The author of [14] describes a cooperation of the mobile robot, which has a motion system similar to the system of upper parts of the human body, with the real operator. This paper considers the problems associated with determining the location of each segment of the robot in outer space. For this purpose the Inertial Measurement Unit (IMU) sensors and known methods to obtain information about the human body motion, such as the Human Motion Capture (Mocap), are used.

In studies which analyze human movement using the IMU sensors, obtaining the actual measurements especially of angles is a major problem, since the IMU measures angular velocity and the actual line speed. However, the appropriate algorithms allow to obtain measurements of the given angles [15].

The development of IMU measurement systems launched studies on the use of not one, but a set of such devices to acquire human motion [16, 17]. This approach allows for unlimited motion parameter measurements regardless of where they occur.

Also computer graphics is one of many applications of information about the parameters of the whole human body motion. The paper [18] presents the method of modeling almost each human muscle in order to represent as realistically as possible the entire human body in motion, also taking into account the invisible muscle movements.

Frequently used methods for the tracking of different human body parts are based on motion parameters or an error estimation, with the use of quaternion Kalman filters [19]. Such approach is reasonable provided that one knows all sensors technical data and kinematic parameters of observed motion. In reality, this is seldom the case and problems arise as which information should be treated as a reference one. What is more, precise determination of human body motion is complicated. Because of that, in this article the authors performed similar research but with the use of a simplified dynamics model of a human arm using known estimators. The presented models, having two degrees of freedom, are frequently applied as the simplest approximation of a human arm, at the same time they suffice for the proper analysis of conducted simulation-based experiments [20–23]. At this preliminary stage of research it is not reasonable to apply more sophisticated mathematical models of human arm [5, 24–26],

*e-mail: artur.babiarz@polsl.pl

as it may dim the picture and lead to improper corollaries. This article rather answers the question if it is possible to determine the state of the object that is the arm model, without the knowledge of kinematics equations. This will allow to avoid dealing with inverse kinematics, which is a complicated tasks [27].

In theoretical considerations state space methods and state space mathematical models are used. Therefore, mathematical models are in the form of differential state equations and algebraic output equation. Moreover, two types of models are considered.

2. Mathematical arm model

First of all, let us introduce two mathematical models of human arm. The mathematical models presented below are the literature-available simplest models of human arm. In many articles devoted to this subject the human arm is modelled as two-segment manipulator capable of motion in a horizontal plane [20, 22]. Frequently, however, there are no consequences of the lack of gravitational force acting in that plane included. It is showed below that in certain conditions the gravity is an important factor influencing the dynamics of the object.

The division into two models, each describing a motion in vertical and horizontal plane respectively, aims into decomposition of the arm joint movement into two separate ones, each with one degree of freedom only [20, 21]. Additionally it is assumed that the shape of each arm segment can be approximated by cuboids [28–30]. Such approach is frequently applied in human motion capture methods [28, 29]. It is also assumed that the arm's muscles do not influence arm's horizontal motion. As a result, the inertias about respective axes are constant and equivalent to the ones of a rotating cuboid, what is a great simplification of the mathematical model. The choice of two degrees of freedom only model is motivated also by the fact, that its behaviour is predictable during operation. With increasing number of degrees of freedom the behaviour prediction is greatly complicated and may be inconclusive.

Model 1

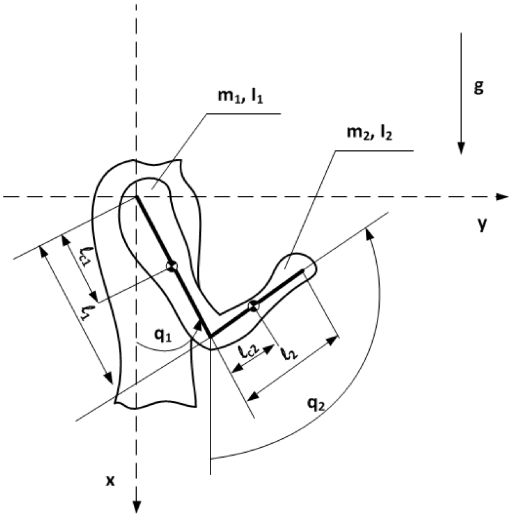

Fig. 1. Two-link arm in vertical plane

The dynamic equation of a two-link arm (Fig. 1) is described by nonlinear state equation:

$$M(\mathbf{q})\,\ddot{\mathbf{q}} + C(\mathbf{q},\dot{\mathbf{q}})\,\dot{\mathbf{q}} + g(\mathbf{q}) = \mathbf{u}, \tag{1}$$

where

$$\mathbf{M} = \begin{bmatrix} c_1 & c_2\cos(q_1 - q_2) \\ c_2\cos(q_1 - q_2) & c_3 \end{bmatrix},$$

$n \times n$ inertia matrix is symmetric and positive definite for each q_i,

$$\mathbf{C} = \begin{bmatrix} 0 & c_2\sin(q_1 - q_2)\,\dot{q}_2 \\ -c_2\sin(q_1 - q_2)\,\dot{q}_1 & 0 \end{bmatrix}$$

Coriolis/centrifugal matrix,

$$\mathbf{g} = \begin{bmatrix} c_4\sin q_1 \\ c_5\sin q_2 \end{bmatrix}$$

is the gravitational forces vector,

$$\mathbf{u} = \begin{bmatrix} u_1 \\ u_2 \end{bmatrix}$$

is the input vector.

$$c_1 = m_1 l_{c1}^2 + m_2 l_1^2 + I_1,$$
$$c_2 = m_2 l_1 l_{c2},$$
$$c_3 = m_2 l_{c2}^2 + I_2,$$
$$c_4 = -(m_1 l_{c1} + m_2 l_1)\,g,$$
$$c_5 = -m_2 l_{c2} g,$$

m is the mass, l the link length, l_c the distance from the joint to the center of mass, I the moment of inertia.

Model 2

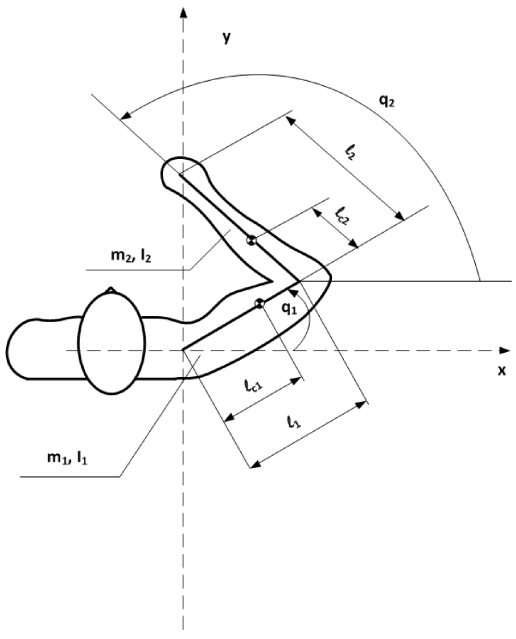

Fig. 2. Two – link arm in horizontal plane [31]

In this case nonlinear state equation has the following form:

$$M(\mathbf{q})\,\ddot{\mathbf{q}} + C(\mathbf{q},\dot{\mathbf{q}})\,\dot{\mathbf{q}} = \mathbf{u} \tag{2}$$

$$\mathbf{M} = \begin{bmatrix} c_1 & c_2 \cos(q_1 - q_2) \\ c_2 \cos(q_1 - q_2) & c_3 \end{bmatrix}$$

is the interia matrix,

$$\mathbf{C} = \begin{bmatrix} 0 & c_2 \sin(q_1 - q_2)\, \dot{q}_2 \\ -c_2 \sin(q_1 - q_2)\, \dot{q}_1 & 0 \end{bmatrix}$$

is the Coriolis/centrifugal matrix,

$$\mathbf{u} = \begin{bmatrix} u_1 \\ u_2 \end{bmatrix}$$

is the input vector.

$$\begin{aligned} c_1 &= m_1 l_{c1}^2 + m_2 l_1^2 + I_1 \\ c_2 &= m_2 l_1 l_{c2} \\ c_3 &= m_2 l_{c2}^2 + I_2 \end{aligned}$$

m is the mass, l the link length, l_c the distance from the joint to the center of mass, I the moment of inertia.

Parameters are presented in Table 1.

Table 1
Parameters of two-link arm

m_1	10 kg
m_2	8 kg
l_1	0.4 m
l_2	0.4 m
l_{c1}	0.2 m
l_{c2}	0.2 m
I_1	0.1667 kgm^2
I_2	0.1333 kgm^2

3. State – space model

Now, we transfer second order differential state Eqs. (1) and (2) into an equivalent set of first order sate equations. The dynamics of model in terms of the state vector $\left[\mathbf{q}^T, \dot{\mathbf{q}}^T\right]^T$ can be expressed as:

Model 1

$$\frac{d}{dt}\begin{bmatrix} \mathbf{q} \\ \dot{\mathbf{q}} \end{bmatrix} = \begin{bmatrix} \dot{\mathbf{q}} \\ M(\mathbf{q})^{-1}\left[u - C(\mathbf{q}, \dot{\mathbf{q}})\, \dot{\mathbf{q}} - g(\mathbf{q})\right] \end{bmatrix}. \quad (3)$$

Model 2

$$\frac{d}{dt}\begin{bmatrix} \mathbf{q} \\ \dot{\mathbf{q}} \end{bmatrix} = \begin{bmatrix} \dot{\mathbf{q}} \\ M(\mathbf{q})^{-1}\left[u - C(\mathbf{q}, \dot{\mathbf{q}})\, \dot{\mathbf{q}}\right] \end{bmatrix}. \quad (4)$$

Now a new set of variables can be assigned to each of the derivatives. In accordance with Eq. (3), the new set of state variables and their equivalences can be drawn as follows:

$$\begin{aligned} x_1 &= q_1, \\ x_2 &= q_2, \\ x_3 &= \dot{x}_1 = \dot{q}_1, \\ x_4 &= \dot{x}_2 = \dot{q}_2. \end{aligned} \quad (5)$$

We can write the general equation of state:

$$\begin{aligned} \dot{\mathbf{x}} &= \mathbf{A}\mathbf{x} + \mathbf{B}\mathbf{u} \\ \mathbf{y} &= \mathbf{C}\mathbf{x} + \mathbf{D}\mathbf{u} \end{aligned} \quad (6)$$

where:

$$\dot{\mathbf{x}} = \begin{bmatrix} \dot{q}_1 \\ \dot{q}_2 \\ \ddot{q}_1 \\ \ddot{q}_2 \end{bmatrix}, \quad \mathbf{x} = \begin{bmatrix} q_1 \\ q_2 \\ \dot{q}_1 \\ \dot{q}_2 \end{bmatrix}, \quad \mathbf{y} = \begin{bmatrix} \ddot{q}_1 \\ \ddot{q}_2 \end{bmatrix}, \quad \mathbf{u} = \begin{bmatrix} u_1 \\ u_2 \end{bmatrix}.$$

Matrixes **A**, **B**, **C**, and **D** are computed using the series expansion linearization method [32]. In accordance with this method we have:

$$\mathbf{A} = \left.\begin{bmatrix} 0 & 0 & 1 & 0 \\ 0 & 0 & 0 & 1 \\ \dfrac{\partial f_1}{\partial x_1} & \dfrac{\partial f_1}{\partial x_2} & \dfrac{\partial f_1}{\partial x_3} & \dfrac{\partial f_1}{\partial x_4} \\ \dfrac{\partial f_2}{\partial x_1} & \dfrac{\partial f_2}{\partial x_2} & \dfrac{\partial f_2}{\partial x_3} & \dfrac{\partial f_2}{\partial x_4} \end{bmatrix}\right|_{\substack{x = x_0 \\ u = u_0}} \quad (7)$$

$$\mathbf{B} = \left.\begin{bmatrix} 0 & 0 \\ 0 & 0 \\ \dfrac{\partial f_1}{\partial u_1} & \dfrac{\partial f_1}{\partial u_2} \\ \dfrac{\partial f_2}{\partial u_1} & \dfrac{\partial f_2}{\partial u_2} \end{bmatrix}\right|_{\substack{x = x_0 \\ u = u_0}} \quad (8)$$

$$\mathbf{C} = \left.\begin{bmatrix} \dfrac{\partial f_1}{\partial x_1} & \dfrac{\partial f_1}{\partial x_2} & \dfrac{\partial f_1}{\partial x_3} & \dfrac{\partial f_1}{\partial x_4} \\ \dfrac{\partial f_2}{\partial x_1} & \dfrac{\partial f_2}{\partial x_2} & \dfrac{\partial f_2}{\partial x_3} & \dfrac{\partial f_2}{\partial x_4} \end{bmatrix}\right|_{\substack{x = x_0 \\ u = u_0}} \quad (9)$$

$$\mathbf{D} = \left.\begin{bmatrix} \dfrac{\partial f_1}{\partial u_1} & \dfrac{\partial f_1}{\partial u_2} \\ \dfrac{\partial f_2}{\partial u_1} & \dfrac{\partial f_2}{\partial u_2} \end{bmatrix}\right|_{\substack{x = x_0 \\ u = u_0}} \quad (10)$$

where x_0, u_0 is the operating point. The elements of **A**, **B**, **C** and **D** matrices after linearization are shown in Appendix A.

4. Linear state observer

In practical applications the use of the state feedback is usually limited by the ability to measure all state variables. In other words, we say that the state variables are not available for measurements. In this case, the application of state observer can be considered. The state observer estimates the state of the process on the grounds of the input and output signal and knowledge of the process model.

The role of the observer can be formally defined as follows:

$$\underset{\widehat{x}(0) \in \Re^n}{\forall} \lim_{t \to \infty} \left\| x(t) - \widehat{x}(t) \right\| \leq \varepsilon, \quad (11)$$

where $x(t)$ is the state, $\widehat{x}(t)$ is the estimated state, while $\varepsilon \geq 0$ is the constant (arbitrarily small). This means that the observer should permit to reproduce the state with possibly small

error. As usually the initial value of the estimated state $\widehat{x}(0)$ is significantly different from the initial value of the unknown state $x(0)$ the occurrence of transient states should be noted. The duration of transient states depends on the type of observer and the selected values of observer gain.

In simulation experiments we shall use the Kalman filter and the particle filter. Therefore, for convenience we recall the Kalman filter algorithm and the particle filter algorithm.

5. Kalman filter

The Kalman filter is a type of the recursive estimation method designed for linear discrete stochastic processes described by the following equations [33–36]:

$$\begin{aligned} x_k &= Fx_{k-1} + Gu_{k-1} + V\nu_{k-1}, \\ y_k &= Hx_k + Ww_k, \end{aligned} \tag{12}$$

where $x_k \in \Re^n$, $u_k \in \Re^l$, $y_k \in \Re^m$ denote respectively the state, input and output (or measurement signal) at the time k, while ν_k and w_k indicate noise (distortion) of the process and measurement noise [37–39].

F, G, V, H, W are given constant matrices of appropriate dimensions.

The first differential equation is the process model, which is partially deterministic and partially random. This a connection between previous state and present state through the matrix. The G matrix is the extortion of state (control), v is the so called process noise (random part). The second equation is the measurement model, where H is a matrix binding the state with the measurement (filter output), and is the measurement noise.

We assume that the noise signals ν and w are uncorrelated sequence of samples with zero expected value:

$$E[\nu] = E[w] = 0. \tag{13}$$

Such signal is defined as a white noise. Dispersion of vector random variables and describes the process covariance matrix Q and the covariance matrix of the measurement R. Hence, we have

$$\begin{aligned} Q &= E\left[\nu^T \nu\right], \\ R &= E\left[w^T w\right]. \end{aligned} \tag{14}$$

The purpose of the Kalman filter is to obtain optimal estimate of the process state in terms of minimizing the covariance matrix:

$$E\left[(x - \widehat{x})^T (x - \widehat{x})\right] \tag{15}$$

Kalman filter algorithm. The Kalman filter algorithm can be presented as follows:

– prediction stage – state and covariance matrix estimation based on the model of the process:

$$\begin{aligned} \widehat{x}_{k|k-1} &= F\widehat{x}_{k-1|k-1} + Gu_{k-1}, \\ P_{k|k-1} &= FP_{k-1|k-1}F^T + VQV^T, \end{aligned} \tag{16}$$

– correction stage (innovation) – state estimate and covariance matrix correction on the basis of the measurement:

$$\begin{aligned} K_k &= P_{k|k-1}H^T \left(HP_{k|k-1}H^T + WRW^T\right)^{-1}, \\ \widehat{x}_{k|k} &= \widehat{x}_{k|k-1} + K_k\left(y_k - H\widehat{x}_{k|k-1}\right), \\ P_{k|k} &= (I - K_k H) P_{k|k-1}. \end{aligned} \tag{17}$$

Presenting the model of Klaman filter with the use of the probabilistic description, it might be written that both ν and w represent Gaussian white noise. Thus, the probability density of these signals can be described by the following relations:

$$\begin{aligned} p(\nu) &\sim N(\nu|\, 0, Q), \\ p(w) &\sim N(w|\, 0, R), \end{aligned} \tag{18}$$

where $\sim$ denotes random variable with the conditional probability distribution, $N(z|\, \mu, \sum)$ is the density function of normal distribution with the variable z, the expected value μ and covariance $\sum$.

Similarly, the description of conditional probabilities allows to define the above model and respectively the probability of state change and the appearance of the given signal is presented in the following way:

$$\begin{aligned} p(x_k|\, x_{k-1}) &\sim N(x_k|\, Fx_{k-1} + Gu_{k-1}, Q) \\ p(y_k|\, x_k) &\sim N(y_k|\, Hx_k, R). \end{aligned} \tag{19}$$

Covariance matrices (depending on the variance of the state vector components) are:

$$\begin{aligned} P_{k|k-1} &= E\left[e^T_{k|k-1} e_{k|k-1}\right], \\ P_{k|k} &= E\left[e^T_{k|k} e_{k|k}\right], \end{aligned} \tag{20}$$

where $P_{k|k-1}$ is the a priori covariance matrix, and $P_{k|k}$ is the a posteriori covariance matrix. Whereas, $e_{k|k-1}$ is the a priori error, and $e_{k|k}$ is the a posteriori error:

$$\begin{aligned} e_{k|k-1} &= x_k - \widehat{x}_{k|k-1}, \\ e_{k|k} &= x_k - \widehat{x}_{k|k}. \end{aligned} \tag{21}$$

It should be pointed out, that these are the differences between the actual state and the estimated value. In practice, the actual state values of x_k are unknown and the covariance matrix is estimated using only the filtration process.

It is also possible to define the density function of conditional probability which constitutes the filtering result and determines the probability of occurrence of the particular process state provided the measurement sequence (output signal) occurs:

$$p(x_k|\, Y_{1:k}) \sim N\left(x_k|\, \widehat{x}_k, P_{k|k}\right), \tag{22}$$

where $Y_{1:k} = \{y_1, y_2, \cdots, y_k\}$ is the set of observations (measurements) in the next moments.

6. The particle filter

Thus, in Kalman filter, taking into account the probability of error (noise measurement, measurement system errors), the state variable vector x_k is estimated on the basis of the system measurement vector y_k in the presence of disturbances.

It could be said, that the system state and the probability of its occurrence are estimated. Simultaneously, it is assumed that the density of the conditional probability density for these systems is subjected to Gaussian white noise.

However, systems models that describe the system properties are often non-linear, and the distribution of noise deviates from Gaussian distribution. Applying the probabilistic approach it can be said that the solution to the filtering problem is determining the conditional probability density $p(X_{1:k}|Y_{1:k})$ a posteriori (called posterior density), where $X_{1:k} = \{x_1, x_2, \cdots, x_k\}$ is the set of the state values in subsequent moments, and $Y_{1:k} = \{y_1, y_2, \cdots, y_k\}$ is the set of system observations. In order to make the proposed solution independent from the full history of the state variables $X_{1:k}$, the recursive calculation of the conditional filtered probability density a posteriori $p(x_k|Y_{1:k})$ (called filtered density) can be used.

Having some a priori knowledge of the studied system, we can describe its dynamics with two equations (just like in case of Kalman filter (Eq. (19)). Equation of state is determined by the a priori distribution of the hidden Markov process $\{x_k\}_{k\in N}$, and the equation of observation (output) $\{y_k\}_{k\in N}$ by the conditional distribution of observations $p(y_k|x_k)$:

$$\begin{aligned} x_k &\sim p(x_k|x_{k-1}), \\ y_k &\sim p(y_k|x_k). \end{aligned} \tag{23}$$

The knowledge of the above distributions allows to use Bayes' rule which combines a priori distributions of unknown states with the probability of a given baseline (follow-up) system. All relevant information concerning the state variable $X_{01:k}$ with the assumption that the observations are known up to the moment k $Y_{1:k}$ of are included in the total a posteriori distribution $p(X_{01:k}|Y_{1:k})$. The idea of the filtration method involves the estimation of the mentioned distribution $p(X_{01:k}|Y_{1:k})$, its characteristics and boundary distribution $p(x_k|Y_{1:k})$.

If the filtered probability density has already been defined, by using it the state variables estimates of the observed system can be determined:

$$\widehat{x}_k = E[x_k|Y_{1:k}] = \int x_k p(x_k|Y_{1:k})\, dx_k. \tag{24}$$

It turns out, however, that as far as the Bayesian inference principles are simple, in practice there occur problems of numerical nature. Only in a few exceptional cases, such as linear Gaussian models and hidden Markov chains defined in a finite state space, a posteriori distribution has analytical form.

In case of multidimensional spaces of hidden variables subjected to disturbances, Monte Carlo methods are the only analytical methods.

The idea of particle filter is based on the presentation of the estimated state variables through a set of random samples (particles) and their assigned weights. The particle filter can be seen as a method of simulation involving the simulation of a large number of potential state variables trajectories. Each of these trajectories is represented at a given discrete time using a single number (particles). Using information obtained from consecutive measurements of each trajectory a weight is assigned, which determines the probability that a given trajectory represents the actual trajectory [40–45].

The function of a particle filter is to generate the possible implementation of the state vector at a given moment, and then assign appropriate weights to these realizations. These realizations together with their assigned weights create the probability density approximations of marginal distribution $p(x_k|Y_{1:k})$, which is a searched solution to the filtration problem.

Particle filter algorithm. In order to determine the marginal distribution $p(x_k|Y_{1:k})$ approximation particle filters use recursive Bayesian estimation:
– prediction stage:

$$p(x_k|Y_{1:k-1}) = \int p(x_k|x_{k-1})\, p(x_{k-1}|Y_{1:k-1})\, dx_{k-1}, \tag{25}$$

where $p(x_k|x_{k-1})$ is determined by the transfer function of the model;
– correction stage:

$$p(x_k|Y_{1:k}) = \frac{p(y_k|x_k)\, p(x_k|Y_{1:k-1})}{p(y_k|Y_{1:k-1})}, \tag{26}$$

where $p(y_k|x_k)$ is the output equation (measurement) of the system model and

$$p(y_k|Y_{1:k}) = \int p(y_{\ k}|x_k)\, p(x_k|Y_{1:k-1})\, dx_k. \tag{27}$$

The searched marginal distribution $p(x_k|Y_{1:k})$ contains all available information at the time k on the hidden state variable.

In general case, due to the lack of the analytical form of the considered density distribution it is necessary to use numerical methods.

In the presented approach for molecular filter design the simulation Monte Carlo method was chosen. This idea is based on the distribution theory. If the random variable x has density distribution p and when for the considered distribution there is a pseudo-random number generator, then the estimator of the probability measurement p is the empirical distribution in form:

$$\widehat{p}(x) = \frac{1}{M}\sum_{i=1}^{M} \delta\left(x - x^i\right), \tag{28}$$

where $\delta(z)$ is the Dirac delta, and the sequence $\left\{x^i\right\}_{i=1}^{M}$ is a sequence of independent samples generated from the distribution p (called perfect Monte Carlo sampling).

If the studied distribution is complex, highly dimensional, non-standard and moreover it is known to an accuracy of the normalization constant, the direct generating of the samples is complex or even impossible. As a result, the method of generating the sample on the basis of the empirical distribution uses the function validity method.

The idea of the particle filter method is to replace the analyzed distribution p with the distribution q (with possibly similar properties), for which there is a pseudo-random number generator. Using q introduced distribution a sample of

independent, random, weighted variables $\left\{x^i, w^i\right\}_{i=1}^{M}$ is generated. In the case of M independent random variables with the density the estimator q probability measure is defined:

$$\widehat{p}\,(x) = \sum_{i=1}^{M} w^i \delta\left(x - x^i\right), \tag{29}$$

where $\sum\limits_{i=1}^{N} w^i = 1, \forall i = 1, 2, \ldots, N \; w^i \geq 0$.

In practice, a direct sampling from the distribution boundary $p\left(x_k \middle| Y_{1:k}\right)$ is not often an easy task, therefore, samples are drawn from the cumulative distribution $p\left(X_{\ 1:k} \middle| Y_{1:k}\right)$, and then values $x_{1:k-1}$ are eliminated. The idea of sequential estimation of distribution $p\left(X_{\ 1:k} \middle| Y_{1:k}\right)$ on the basis of Sequential Importance Sampling, (SIS) is to recursively estimate the $\widehat{p}\left(X_{\ 1:k} \middle| Y_{1:k}\right)$ without changing the history of states $\left\{x_{1:k}^i\right\}_{i=1}^{M}$. Then the approximation $p\left(x_k \middle| Y_{1:k}\right)$ is expressed by the following equation:

$$p\left(x_k \middle| Y_{1:k}\right) = \sum_{i=1}^{M} \widetilde{w}_k^i \delta\left(x_k - x_k^i\right). \tag{30}$$

Taking into consideration the above dependence in a recursive Bayesian algorithm (Eq. (25)–(27)) we get:

$$p\left(x_k \middle| Y_{1:k}\right) = p\left(y_k \middle| x_k\right) \sum_{i=1}^{M} \widetilde{w}_{k-1}^i p\left(x_k \middle| x_{k-1}^i\right). \tag{31}$$

From the above formula it follows that the set of samples representing approximation $p\left(x_k \middle| Y_{1:k}\right)$ is generated by the samples $p\left(x_k \middle| x_{k-1}^i\right)$, that is:

$$x_k^i \sim p\left(x_k \middle| x_{k-1}^i\right), \; i = 1, 2, \ldots, M. \tag{32}$$

The particle filter – SIS algorithm

1. For $k = 0$ (initialization):

$$x_0^i \sim q\left(x_0\right), \widetilde{w}_0^i = \frac{1}{M}, \; i = 1, 2, \ldots, M$$

2. For $k = 1, 2, \ldots, N$

– generate (prediction):

$$x_k^i \sim p\left(x_k \middle| x_{k-1}^i\right), \; i = 1, 2, \ldots, M$$

– we set the weight of particles (correction):

$$w_k^i = p\left(y_{\ k} \middle| x_{k-1}^i\right) \widetilde{w}_{k-1}^i, \; i = 1, 2, \ldots, M$$

– we normalize the importance weights of particles:

$$\widetilde{w}_k^i = \frac{w_k^i}{\sum\limits_{i=1}^{M} w_k^i}, \; i = 1, 2, \ldots, M$$

– we determine an estimate of the system:

$$\widehat{x}_k = \sum_{i=1}^{M} \widetilde{w}_k^i x_k^i.$$

In practice, after several iterations of the SIS algorithm it turns out that all validity coefficients except one receive the values negligibly low (close to zero) – the so called degeneracy phenomenon of the sample appears. This phenomenon causes that the significant computational effort is spent on the molecules, whose contribution to the approximation $p\left(x_k \middle| Y_{1:k}\right)$ is almost equal to zero. Therefore, the additional sampling in order to "renew" trajectory (called resampling) is introduced to the algorithm. The basic resampling procedure consists of sampling value M from the available population of molecules. Sampling takes place in accordance with standardized weights determined during the algorithm and generally involves mapping a set of molecules M with different weights into the new set of particles M with equal weights $\left\{x_k^i, \widetilde{w}_k^i\right\}_{i=1}^{M} \rightarrow \left\{\widetilde{x}_k^i, \frac{1}{M}\right\}_{i=1}^{M}$.

In the literature there are at least a few methods known for resampling: multinomial resampling, residual resampling, systematic resampling.

7. The simulation experiments

In this section we present results of simulation experiments. In simulation experiments model 1 was linearized at four operating points $\left(\mathbf{x}_0^i, \mathbf{u}_0^i\right) = \left(\left[x_{10}^i; x_{20}^i; x_{30}^i; x_{40}^i\right], \left[u_{10}^i, u_{20}^i\right]\right)$, $i = 1, 2, 3, 4$. Therefore, operating points are of the following form:

$$\left(\mathbf{x}_0^1, \mathbf{u}_0^1\right) = \left([0; 0; 0; 0], [0; 0]\right),$$

$$\left(\mathbf{x}_0^2, \mathbf{u}_0^2\right) = \left([0,768; 0,785; 0; 0], [0; 0]\right),$$

$$\left(\mathbf{x}_0^3, \mathbf{u}_0^3\right) = \left([0,785; 0,785; 0; 0], [0; 0]\right),$$

$$\left(\mathbf{x}_0^4, \mathbf{u}_0^4\right) = \left([0,017; 0,017; 0; 0], [0; 0]\right).$$

The operating point $\left(\mathbf{x}_0^1, \mathbf{u}_0^1\right)$ is an equilibrium point. The remaining operating points are arbitrarily selected ones.

The state variables x_1, x_2 are expressed in radians $[rad]$, x_3, x_4 are expressed in $\left[\frac{\text{rad}}{\text{s}}\right]$ and control are in Newton-meters [Nm].

In order to observe the state vector two estimates methods are used: the Kalman filter and the particle filter.

Kalman filter parameters are as follows: the starting point $x\left(0\right) = \left[0.5 \text{ rad}; \; 0.5 \text{ rad}; \; 0 \; \frac{\text{rad}}{\text{s}}; \; 0 \; \frac{\text{rad}}{\text{s}}\right]$, matrices $\mathbf{Q} = diag\left(0.00001\right)$, $\mathbf{R} = diag\left(0.01\right)$. Whereas, the particle filter works with the following parameters: number of particles 200, starting point $x\left(0\right) = \left[0.5 \text{ rad}; \; 0.5 \text{ rad}; \; 0 \; \frac{\text{rad}}{\text{s}}; \; 0 \; \frac{\text{rad}}{\text{s}}\right]$, generation of particles – uniform distribution on the interval $[x\left(0\right) - 0.5; x\left(0\right) + 0.5]$.

For all simulation experiments the discretization step $dt = 0.001s$ and number of samples $T = 10000$ were assumed.

The operating point $\left(\mathbf{x}_0^1, \mathbf{u}_0^1\right)$

Matrices $\mathbf{A}$ and $\mathbf{C}$ obtained by linearization around the operating point $\left(\mathbf{x}_0^1, \mathbf{u}_0^1\right) = \left([0; 0; 0; 0], [0; 0]\right)$ have the following form:

$$\mathbf{A} = \begin{bmatrix} 0 & 0 & 1 & 0 \\ 0 & 0 & 0 & 1 \\ 54,09 & 23,50 & 0 & 0 \\ 76,36 & -67,79 & 0 & 0 \end{bmatrix}$$

$$\mathbf{C} = \begin{bmatrix} 54,09 & 23,50 & 0 & 0 \\ 76,36 & -67,79 & 0 & 0 \end{bmatrix}$$

It can be easly computed that since $n = 4$:

$$rank \begin{bmatrix} C \\ CA \\ \vdots \\ CA^{n-1} \end{bmatrix} = rank \begin{bmatrix} C \\ CA \\ CA^2 \\ CA^3 \end{bmatrix} = 4.$$

Hence, object with matrices **A**, **C** is observable.

Only these two matrices are important due to the observability of the dynamical system. Of course, the arm at such operating point is observable.

The Figs. 3–5 present the $q_1, \dot{q}_1, \ddot{q}_1$ simulated waveforms and their estimation.

The Figs. 6–8 present the $q_2, \dot{q}_2, \ddot{q}_2$ simulated waveforms and their estimation.

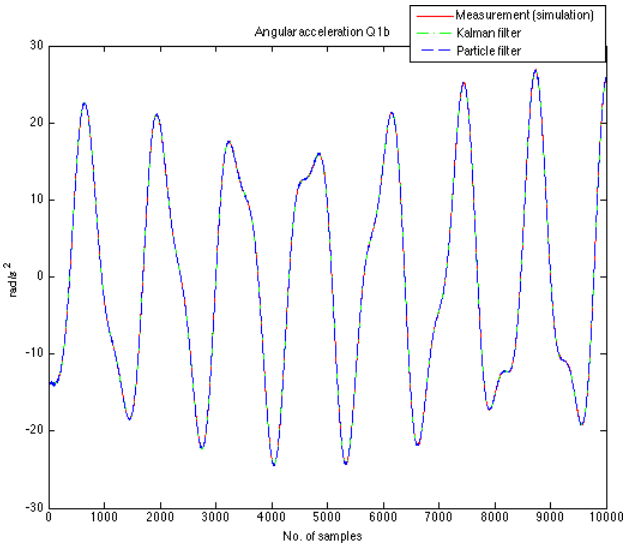

Fig. 5. The $\ddot{q}_1$ angular acceleration for a point $\left(\mathbf{x}_0^1, \mathbf{u}_0^1\right)$

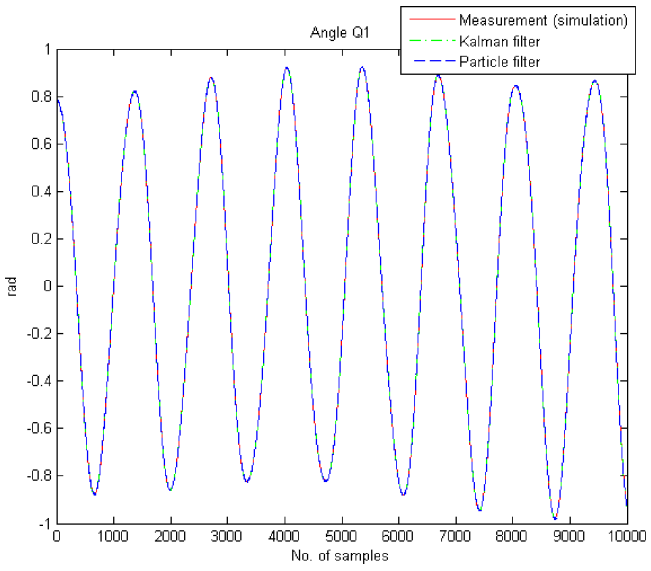

Fig. 3. The q_1 angle for the point $\left(\mathbf{x}_0^1, \mathbf{u}_0^1\right)$

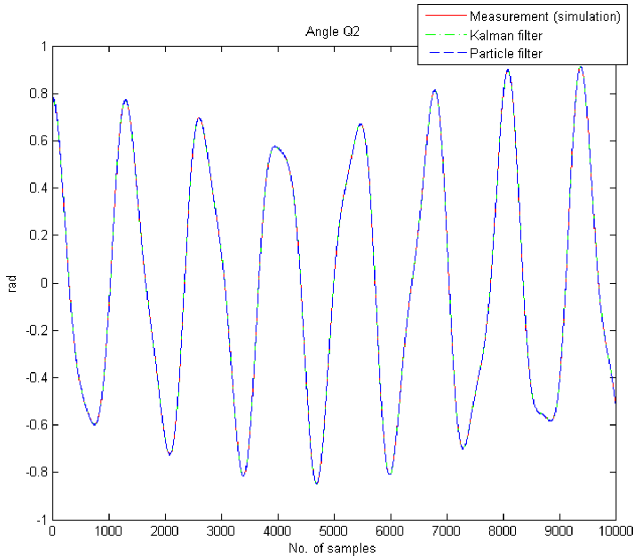

Fig. 6. The q_2 angle for the point $\left(\mathbf{x}_0^1, \mathbf{u}_0^1\right)$

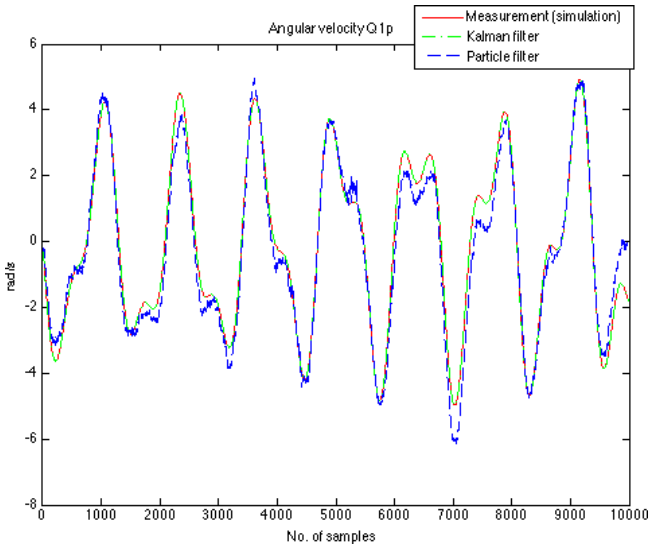

Fig. 4. The $\dot{q}_1$ angular velocity for a point $\left(\mathbf{x}_0^1, \mathbf{u}_0^1\right)$

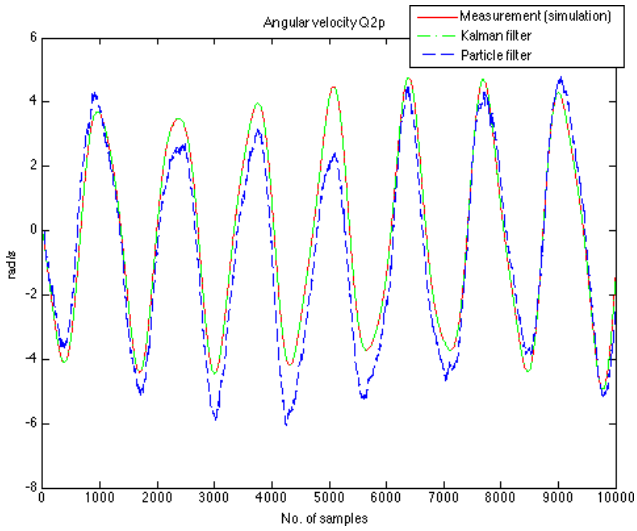

Fig. 7. The $\dot{q}_2$ angular velocity for a point $\left(\mathbf{x}_0^1, \mathbf{u}_0^1\right)$

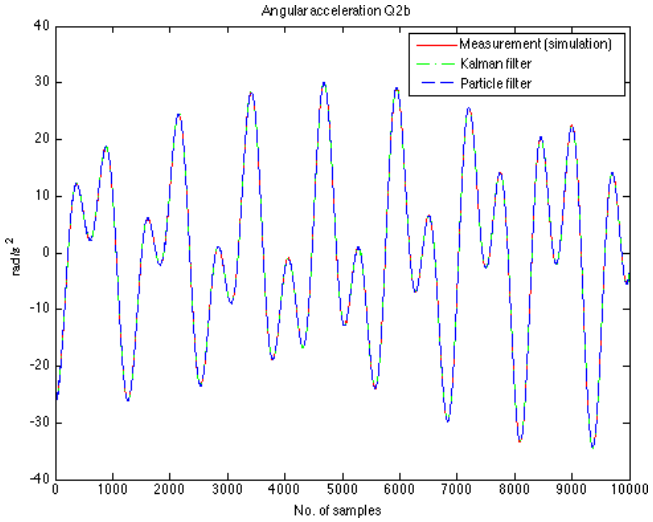

Fig. 8. The $\ddot{q}_2$ angular acceleration for a point $\left(\mathbf{x}_0^1, \mathbf{u}_0^1\right)$

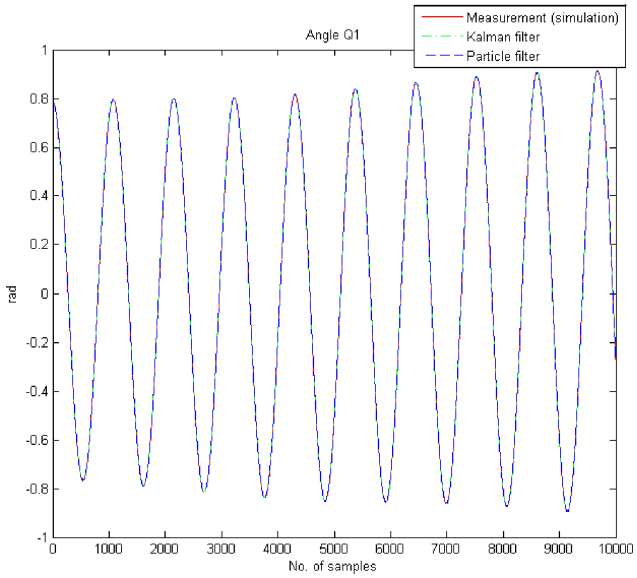

Fig. 9. The q_1 angle for the point $\left(\mathbf{x}_0^2, \mathbf{u}_0^2\right)$

The operating point $\left(\mathbf{x}_0^2, \mathbf{u}_0^2\right)$

Matrices **A** and **C** obtained by linearization around the operating point $\left(\mathbf{x}_0^2, \mathbf{u}_0^2\right) = \left([0,768; 0,785; 0; 0], [0; 0]\right)$ have the following form

$$\mathbf{A} = \begin{bmatrix} 0 & 0 & 1 & 0 \\ 0 & 0 & 0 & 1 \\ -39,31 & 17,02 & 0 & 0 \\ 56,00 & -49,02 & 0 & 0 \end{bmatrix}$$

$$\mathbf{C} = \begin{bmatrix} -39,31 & 17,02 & 0 & 0 \\ 56,00 & -49,02 & 0 & 0 \end{bmatrix}$$

It can be easly computed that since $n = 4$:

$$rank \begin{bmatrix} C \\ CA \\ \vdots \\ CA^{n-1} \end{bmatrix} = rank \begin{bmatrix} C \\ CA \\ CA^2 \\ CA^3 \end{bmatrix} = 4.$$

Hence, object with matrices **A**, **C** is observable.

Comparisons of the simulated measurements and obtained estimates $q_1, \dot{q}_1, \ddot{q}_1$ are presented in Figs. 9–11.

Comparing the accuracy of the angular velocity waveforms $\dot{q}_1$ and $\dot{q}_2$, it can be concluded that here occur are the most major errors (Figs. 10 and 13). The remaining values are almost identical (Figs. 12 and 14).

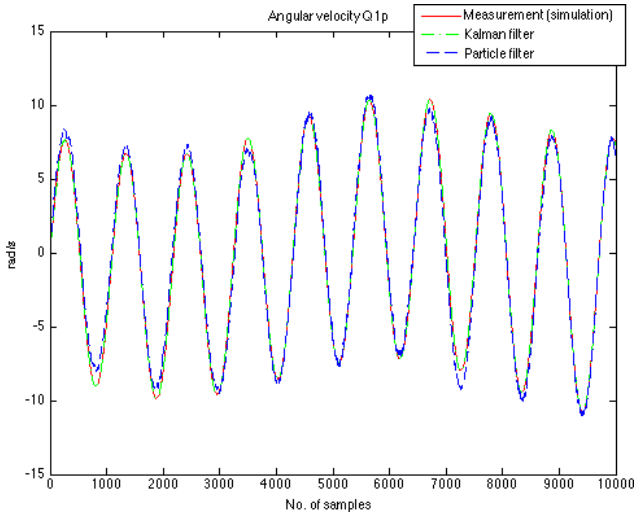

Fig. 10. The $\dot{q}_1$ angular velocity for a point $\left(\mathbf{x}_0^2, \mathbf{u}_0^2\right)$

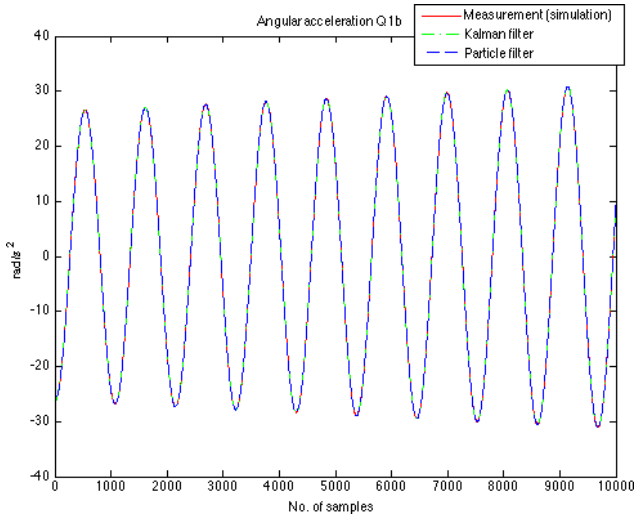

Fig. 11. The $\ddot{q}_1$ angular acceleration for a point $\left(\mathbf{x}_0^2, \mathbf{u}_0^2\right)$

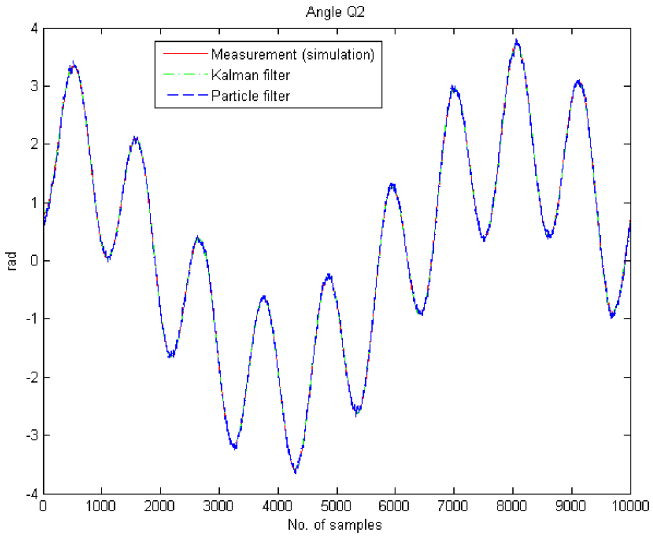

Fig. 12. The q_2 angle for the point $\left(\mathbf{x}_0^2, \mathbf{u}_0^2\right)$

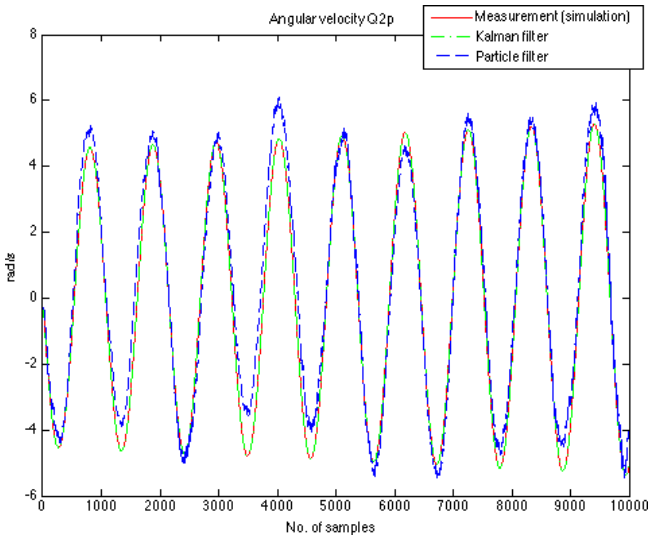

Fig. 13. The $\dot{q}_2$ angular velocity for a point $\left(\mathbf{x}_0^2, \mathbf{u}_0^2\right)$

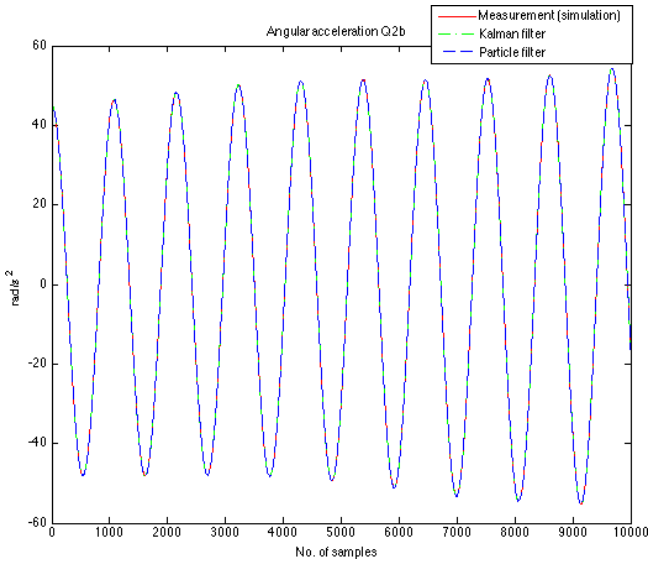

Fig. 14. The $\ddot{q}_2$ angular acceleration for a point $\left(\mathbf{x}_0^2, \mathbf{u}_0^2\right)$

The operating point $\left(\mathbf{x}_0^3, \mathbf{u}_0^3\right)$

Matrices $\mathbf{A}$ and $\mathbf{C}$ obtained by linearization around the operating point $\left(\mathbf{x}_0^3, \mathbf{u}_0^3\right) = \left([0,785; 0,785; 0; 0], [0; 0]\right)$ have the following form

$$\mathbf{A} = \begin{bmatrix} 0 & 0 & 1 & 0 \\ 0 & 0 & 0 & 1 \\ -38,25 & 16,61 & 0 & 0 \\ 53,99 & -47,94 & 0 & 0 \end{bmatrix}$$

$$\mathbf{C} = \begin{bmatrix} -38,25 & 16,61 & 0 & 0 \\ 53,99 & -47,94 & 0 & 0 \end{bmatrix}$$

It can be easly computed that since $n = 4$:

$$rank \begin{bmatrix} C \\ CA \\ \vdots \\ CA^{n-1} \end{bmatrix} = rank \begin{bmatrix} C \\ CA \\ CA^2 \\ CA^3 \end{bmatrix} = 4.$$

Hence, object with matrices $\mathbf{A}$, $\mathbf{C}$ is observable.

Figures 15–17 show the $q_1, \dot{q}_1, \ddot{q}_1$ simulated waveforms and their estimation.

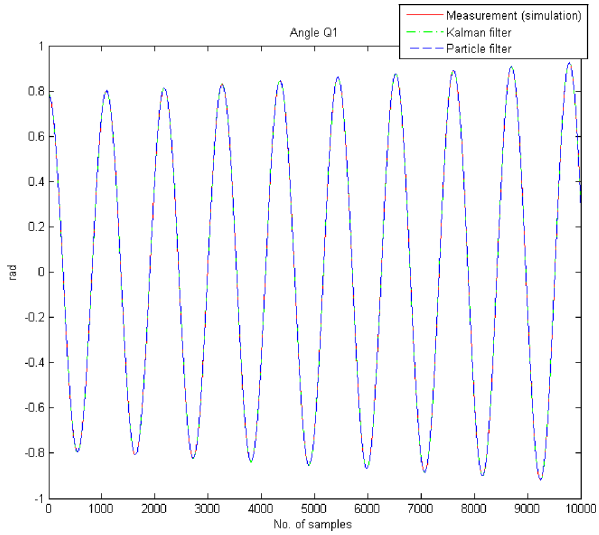

Fig. 15. The q_1 angle for the point $\left(\mathbf{x}_0^3, \mathbf{u}_0^3\right)$

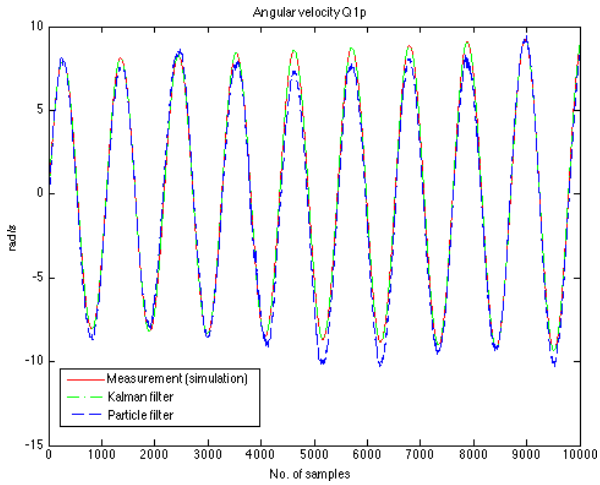

Fig. 16. The $\dot{q}_1$ angular velocity for a point $\left(\mathbf{x}_0^3, \mathbf{u}_0^3\right)$

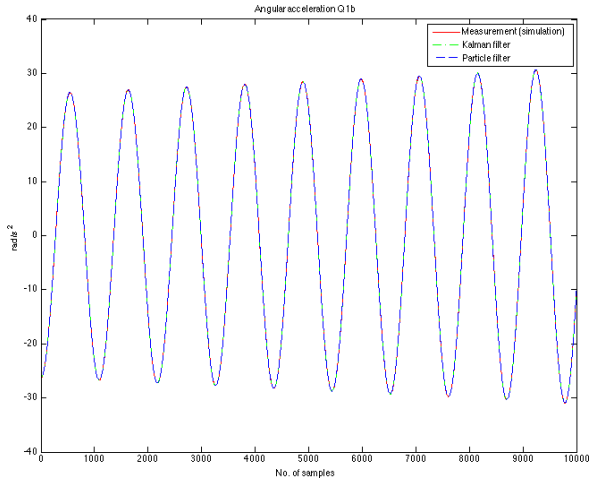

Fig. 17. The $\ddot{q}_1$ angular acceleration for a point $\left(\mathbf{x}_0^3, \mathbf{u}_0^3\right)$

Figures 18–20 present the $q_2, \dot{q}_2, \ddot{q}_2$ simulated waveforms and their estimation.

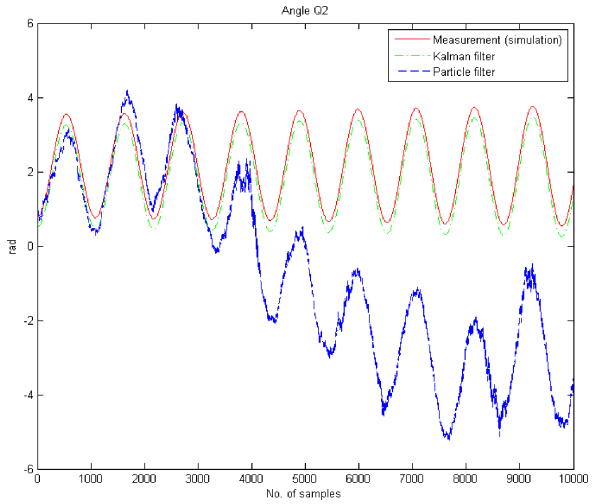

Fig. 18. The q_2 angle for the point $\left(\mathbf{x}_0^3, \mathbf{u}_0^3\right)$

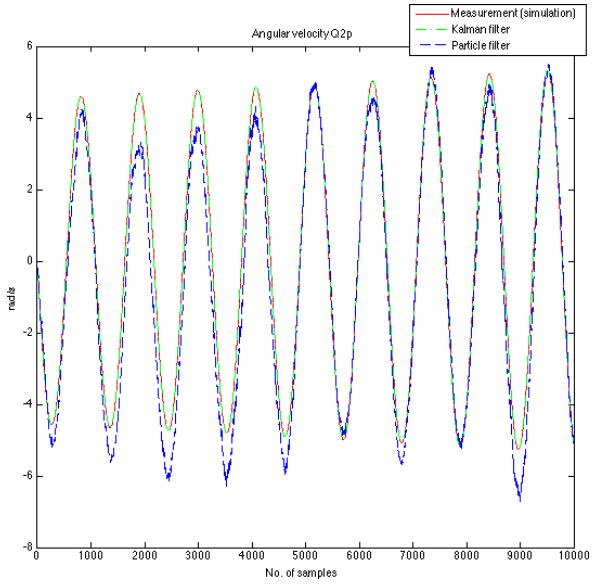

Fig. 19. The $\dot{q}_2$ angular velocity for a point $\left(\mathbf{x}_0^3, \mathbf{u}_0^3\right)$

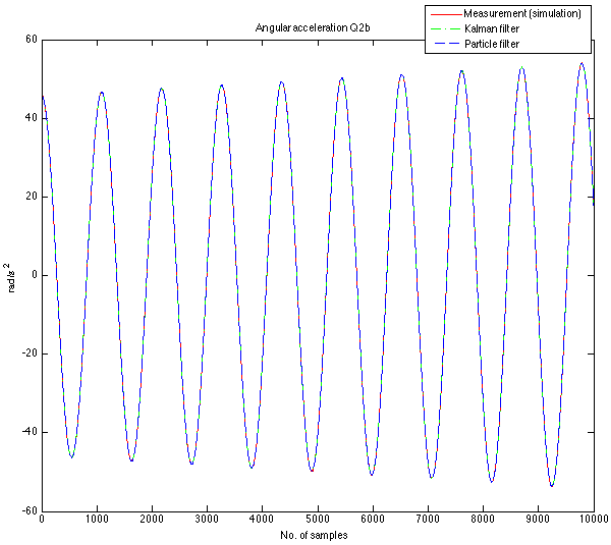

Fig. 20. The $\ddot{q}_2$ angular acceleration for a point $\left(\mathbf{x}_0^3, \mathbf{u}_0^3\right)$

In Fig. 18 a totally inaccurate q_2 angle estimation can be observed. Probably due to the selected operating point, because in the dynamics model there are differences in angles. This can cause unpredictable behavior of the simulated object.

The operating point $\left(\mathbf{x}_0^4, \mathbf{u}_0^4\right)$

Matrices $\mathbf{A}$ and $\mathbf{C}$ obtained by linearization around the operating point $\left(\mathbf{x}_0^4, \mathbf{u}_0^4\right) = \left([0,017; 0,017; 0; 0], [0; 0]\right)$ have the following form

$$\mathbf{A} = \begin{bmatrix} 0 & 0 & 1 & 0 \\ 0 & 0 & 0 & 1 \\ -46,84 & 20,35 & 0 & 0 \\ 66,13 & -58,71 & 0 & 0 \end{bmatrix}$$

$$\mathbf{C} = \begin{bmatrix} -46,84 & 20,35 & 0 & 0 \\ 66,13 & -58,71 & 0 & 0 \end{bmatrix}$$

It can be easly computed that since $n = 4$:

$$rank \begin{bmatrix} C \\ CA \\ \vdots \\ CA^{n-1} \end{bmatrix} = rank \begin{bmatrix} C \\ CA \\ CA^2 \\ CA^3 \end{bmatrix} = 4$$

Hence, object with matrices $\mathbf{A}$, $\mathbf{C}$ is observable.

The last operating point was selected in a way so that there are no singularities associated with the trigonometric functions, and thus with the dynamic model of the object. Graphs of q_1 angles, $\dot{q}_1$ velocities and $\ddot{q}_1$ accelerations are illustrated in the Figs. 21–23.

As for the second operating point also here are the most major inaccurate angular velocities (Figs. 22 and 25). For other motion parameters highly accurate results from the Kalman filter and the particle filter (Figs. 24 and 26) were obtained.

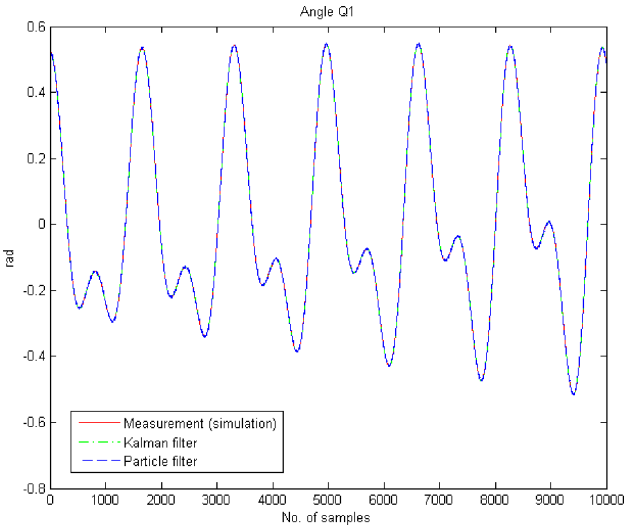

Fig. 21. The q_1 angle for the point $\left(\mathbf{x}_0^4, \mathbf{u}_0^4\right)$

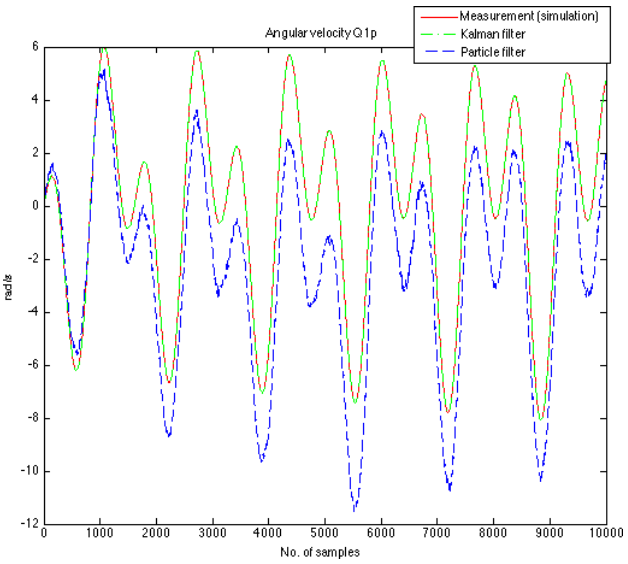

Fig. 22. The $\dot{q}_1$ angular velocity for a point $\left(\mathbf{x}_0^4, \mathbf{u}_0^4\right)$

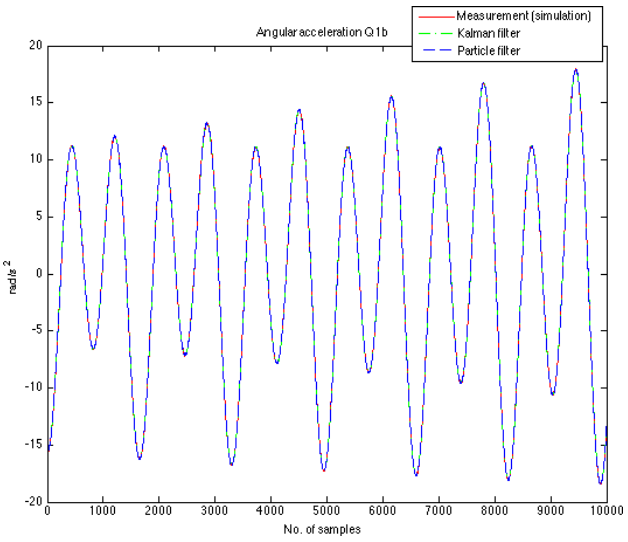

Fig. 23. The $\ddot{q}_1$ angular acceleration for a point $\left(\mathbf{x}_0^4, \mathbf{u}_0^4\right)$

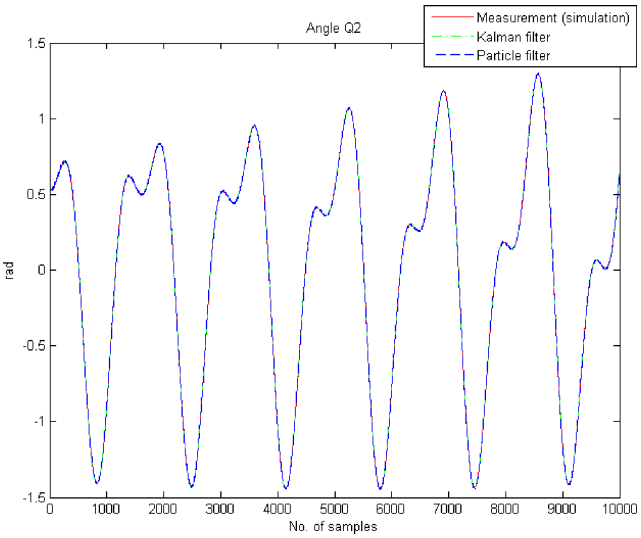

Fig. 24. The q_2 angle for the point $\left(\mathbf{x}_0^4, \mathbf{u}_0^4\right)$

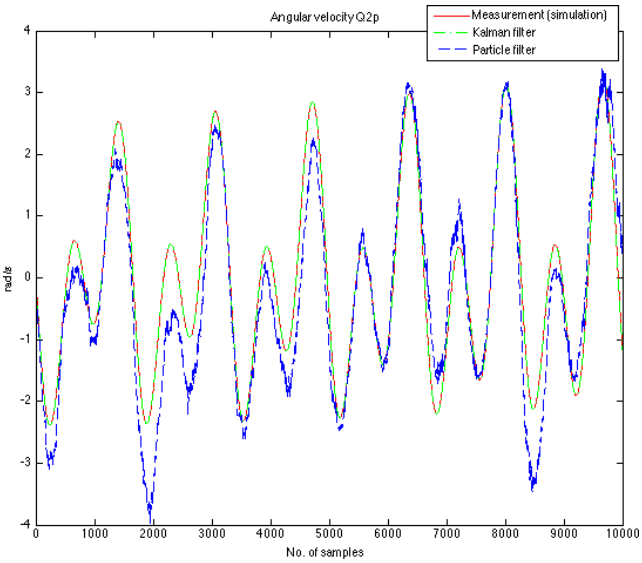

Fig. 25. The $\dot{q}_2$ angular velocity for a point $\left(\mathbf{x}_0^4, \mathbf{u}_0^4\right)$

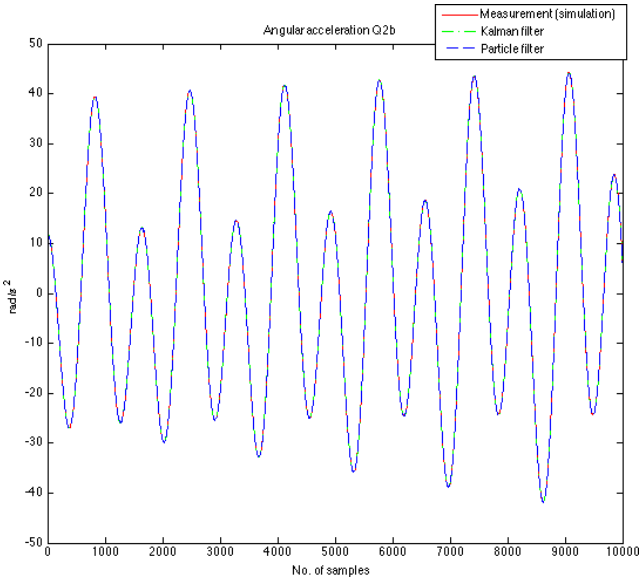

Fig. 26. The $\ddot{q}_2$ angular acceleration for a point $\left(\mathbf{x}_0^4, \mathbf{u}_0^4\right)$

Finally, it should be pointed out that unfortunately, the linearized model 2 at the same operating points as model 1 is a non-observable object.

Matrices **A** and **C** obtained by linearization around the all operating point, every time, have the following form

$$\mathbf{A} = \begin{bmatrix} 0 & 0 & 1 & 0 \\ 0 & 0 & 0 & 1 \\ 0 & 0 & 0 & 0 \\ 0 & 0 & 0 & 0 \end{bmatrix}, \qquad \mathbf{C} = \begin{bmatrix} 0 & 0 & 0 & 0 \\ 0 & 0 & 0 & 0 \end{bmatrix}.$$

It can be easly computed that since $n = 4$:

$$rank \begin{bmatrix} C \\ CA \\ \vdots \\ CA^{n-1} \end{bmatrix} = rank \begin{bmatrix} C \\ CA \\ CA^2 \\ CA^3 \end{bmatrix} \neq 4$$

Therefore, an object with matrices **A**, **C** is non-observable.

As a consequence of this fact it was impossible to generate the simulation data and its estimation or the proposed estimators did not comply with their role. That is why no results of simulation experiments have been presented. Unobservability of a model, follows from mechanical interpretation of the arm.

8. Summary

The basic premise of simulations results was to obtain information about the values of the angles of rotation and angular velocity based only on simulated (measured) angular acceleration. The results of simulation experiments are presented for the characteristic operating points, in which a human hand, without any signals from the muscles, is located in the singular points arising from the dynamics model. On the other hand, the zero control signals were assumed, due to the fact that the measurement of human muscle power for any type of movement is rather a difficult matter. The simulations allow deducing the following conclusion. To measure the actual movement of the object should suffice only accelerometers, not IMU sensors [46].

Moreover, it should be stressed that a very simple model of human arm was used. However, on this stage it could be concluded that singularities occur in a very small environment of a given point, where estimation is inaccurate. That is why the construction of the arm state vector, which has seven degrees of freedom should allow to avoid these points. On the other hand, the accurate reproduction of a real human movement is rather very difficult, because unlike the sensors we are not able to detect these peculiarities.

In terms of future research authors aim to analyze models with more degrees of freedom.

Appendix A

The elements of **A**, **B**, **C** and **D** matrices for Model 1.

$$\ddot{q}_1(q,\dot{q},u) = f_1(q,\dot{q},u) = \frac{u_1}{c_1} - \frac{d_1\cos(q_1-q_2)\,u_2}{c_3 - c_2 d_1\cos^2(q_1-q_2)}$$
$$+\frac{d_1^2\cos^2(q_1-q_2)\,u_1}{c_3 - c_2 d_1\cos^2(q_1-q_2)} - \frac{d_1 d_2 c_2\sin(q_1)\cos(q_1-q_2)}{c_3 - c_2 d_1\cos^2(q_1-q_2)} - \frac{d_1 c_2\sin(q_1-q_2)\cos(q_1-q_2)\,\dot{q}_1^2}{c_3 - c_2 d_1\cos^2(q_1-q_2)}$$
$$+\frac{d_1 c_5\sin(q_2)\cos(q_1-q_2)}{c_3 - c_2 d_1\cos^2(q_1-q_2)} - \frac{d_1^2 c_2\sin(q_1-q_2)\cos^2(q_1-q_2)\,\dot{q}_2^2}{c_3 - c_2 d_1\cos^2(q_1-q_2)} - d_1\sin(q_1-q_2)\,\dot{q}_2^2 - d_2\sin(q_1),$$

$$\ddot{q}_2(q,\dot{q},u) = f_2(q,\dot{q},u) = \frac{u_2}{c_3 - c_2 d_1\cos^2(q_1-q_2)} - \frac{d_1\cos(q_1-q_2)\,u_1}{c_3 - c_2 d_1\cos^2(q_1-q_2)}$$
$$+\frac{d_2 c_2\sin(q_1)}{c_3 - c_2 d_1\cos^2(q_1-q_2)} + \frac{c_2\sin(q_1-q_2)\,\dot{q}_1^2}{c_3 - c_2 d_1\cos^2(q_1-q_2)} - \frac{c_5\sin(q_2)}{c_3 - c_2 d_1\cos^2(q_1-q_2)}$$
$$+\frac{d_1 c_2\sin(q_1-q_2)\cos(q_1-q_2)\,\dot{q}_2^2}{c_3 - c_2 d_1\cos^2(q_1-q_2)},$$

$$d_1 = \frac{c_2}{c_1},$$

$$d_2 = \frac{c_4}{c_1},$$

$$\frac{\partial f_1}{\partial q_1} = \frac{d_1 c_3 u_2 \sin(q_1-q_2)}{(c_3 - d_1 c_2 \cos^2(q_1-q_2))^2} + \frac{d_1^2 c_2 u_2 \sin(q_1-q_2)\cos^2(q_1-q_2)}{(c_3 - d_1 c_2 \cos^2(q_1-q_2))^2} - \frac{2d_1^2 c_3 u_1 \sin(q_1-q_2)\cos(q_1-q_2)}{(c_3 - d_1 c_2 \cos^2(q_1-q_2))^2}$$

$$- \frac{d_1 d_2 c_2 c_3 \cos(q_1)\cos(q_1-q_2)}{(c_3 - d_1 c_2 \cos^2(q_1-q_2))^2} + \frac{d_1^2 d_2 c_2^2 \cos(q_1)\cos^3(q_1-q_2)}{(c_3 - d_1 c_2 \cos^2(q_1-q_2))^2} + \frac{d_1 d_2 c_2 c_3 \sin(q_1)\sin(q_1-q_2)}{(c_3 - d_1 c_2 \cos^2(q_1-q_2))^2}$$

$$+ \frac{d_1^2 d_2 c_2^2 \sin(q_1)\sin(q_1-q_2)\cos^2(q_1-q_2)}{(c_3 - d_1 c_2 \cos^2(q_1-q_2))^2} - \frac{d_1 c_2 c_3 \dot{q}_1^2 \cos^2(q_1-q_2)}{(c_3 - d_1 c_2 \cos^2(q_1-q_2))^2} + \frac{d_1^2 c_2^2 \dot{q}_1^2 \cos^4(q_1-q_2)}{(c_3 - d_1 c_2 \cos^2(q_1-q_2))^2}$$

$$+ \frac{d_1 c_2 c_3 \dot{q}_1^2 \sin^2(q_1-q_2)}{(c_3 - d_1 c_2 \cos^2(q_1-q_2))^2} + \frac{d_1^2 c_2^2 \dot{q}_1^2 \sin^2(q_1-q_2)\cos^2(q_1-q_2)}{(c_3 - d_1 c_2 \cos^2(q_1-q_2))^2} - \frac{d_1 c_3 c_5 \sin(q_2)\sin(q_1-q_2)}{(c_3 - d_1 c_2 \cos^2(q_1-q_2))^2}$$

$$- \frac{2d_1^2 c_2 c_5 \sin(q_2)\cos^3(q_1-q_2)}{(c_3 - d_1 c_2 \cos^2(q_1-q_2))^2} + \frac{d_1^2 c_2 c_5 \sin(q_2)\sin(q_1-q_2)\cos^2(q_1-q_2)}{(c_3 - d_1 c_2 \cos^2(q_1-q_2))^2} - \frac{d_1^2 c_2 c_3 \dot{q}_2^2 \cos^3(q_1-q_2)}{(c_3 - d_1 c_2 \cos^2(q_1-q_2))^2}$$

$$+ \frac{d_1^3 c_2^2 \dot{q}_2^2 \cos^5(q_1-q_2)}{(c_3 - d_1 c_2 \cos^2(q_1-q_2))^2} + \frac{2d_1^2 c_2 c_3 \dot{q}_2^2 \sin^2(q_1-q_2)\cos(q_1-q_2)}{(c_3 - d_1 c_2 \cos^2(q_1-q_2))^2} - d_1 \dot{q}_2^2 \cos(q_1-q_2) - d_2 \cos(q_1)$$

$$\frac{\partial f_1}{\partial q_2} = \frac{-d_1 u_2 c_3 \sin(q_1-q_2)}{(c_3 - d_1 c_2 \cos^2(q_1-q_2))^2} - \frac{d_1^2 c_2 u_2 \sin(q_1-q_2)\cos^2(q_1-q_2)}{(c_3 - d_1 c_2 \cos^2(q_1-q_2))^2} - \frac{2d_1^2 c_2 c_3 u_1 \sin(q_1-q_2)\cos(q_1-q_2)}{(c_3 - d_1 c_2 \cos^2(q_1-q_2))^2}$$

$$+ \frac{4d_1^3 c_2 u_1 \sin(q_1-q_2)\cos^3(q_1-q_2)}{(c_3 - d_1 c_2 \cos^2(q_1-q_2))^2} - \frac{d_1 d_2 c_2 c_3 \sin(q_1)\sin(q_1-q_2)}{(c_3 - d_1 c_2 \cos^2(q_1-q_2))^2} - \frac{d_1^2 d_2 c_2^2 \sin(q_1)\sin(q_1-q_2)\cos^2(q_1-q_2)}{(c_3 - d_1 c_2 \cos^2(q_1-q_2))^2}$$

$$+ \frac{d_1 c_2 c_3 \dot{q}_1^2 \cos^2(q_1-q_2)}{(c_3 - d_1 c_2 \cos^2(q_1-q_2))^2} - \frac{d_1^2 c_2^2 \dot{q}_1^2 \cos^4(q_1-q_2)}{(c_3 - d_1 c_2 \cos^2(q_1-q_2))^2} - \frac{d_1 c_2 c_3 \dot{q}_1^2 \sin^2(q_1-q_2)}{(c_3 - d_1 c_2 \cos^2(q_1-q_2))^2}$$

$$- \frac{d_1^2 c_2^2 \dot{q}_1^2 \sin^2(q_1-q_2)\cos^2(q_1-q_2)}{(c_3 - d_1 c_2 \cos^2(q_1-q_2))^2} + \frac{d_1 c_3 c_5 \cos(q_2)\cos(q_1-q_2)}{(c_3 - d_1 c_2 \cos^2(q_1-q_2))^2} - \frac{d_1^2 c_2 c_5 \cos(q_2)\cos(q_1-q_2)}{(c_3 - d_1 c_2 \cos^2(q_1-q_2))^2}$$

$$+ \frac{d_1 c_3 c_5 \sin(q_2)\sin(q_1-q_2)}{(c_3 - d_1 c_2 \cos^2(q_1-q_2))^2} + \frac{d_1^2 c_2 c_5 \sin(q_2)\sin(q_1-q_2)\cos^2(q_1-q_2)}{(c_3 - d_1 c_2 \cos^2(q_1-q_2))^2} + \frac{d_1^2 c_2 c_5 \dot{q}_2^2 \cos^3(q_1-q_2)}{(c_3 - d_1 c_2 \cos^2(q_1-q_2))^2}$$

$$- \frac{d_1^3 c_2^2 \dot{q}_2^2 \cos^5(q_1-q_2)}{(c_3 - d_1 c_2 \cos^2(q_1-q_2))^2} - \frac{2d_1^2 c_2 c_3 \dot{q}_2^2 \sin^2(q_1-q_2)\cos(q_1-q_2)}{(c_3 - d_1 c_2 \cos^2(q_1-q_2))^2} + d_1 \dot{q}_2^2 \cos(q_1-q_2),$$

$$\frac{\partial f_1}{\partial \dot{q}_1} = \frac{-2d_1 c_2 \dot{q}_1 \sin(q_1-q_2)\cos(q_1-q_2)}{c_3 - d_1 c_2 \cos^2(q_1-q_2)},$$

$$\frac{\partial f_1}{\partial \dot{q}_2} = \frac{-2d_1^2 c_2 \dot{q}_2 \sin(q_1-q_2)\cos^2(q_1-q_2)}{c_3 - d_1 c_2 \cos^2(q_1-q_2)} - 2d_1 \dot{q}_2 \sin(q_1-q_2),$$

$$\frac{\partial f_1}{\partial u_1} = \frac{1}{c_1} + \frac{d_1^2 \cos^2(q_1-q_2)}{c_3 - d_1 c_2 \cos^2(q_1-q_2)},$$

$$\frac{\partial f_1}{\partial u_2} = \frac{-d_1 \cos(q_1-q_2)}{c_3 - d_1 c_2 \cos^2(q_1-q_2)},$$

$$\frac{\partial f_2}{\partial q_1} = -\frac{2d_1c_2\sin(q_1-q_2)\cos(q_1-q_2)}{(c_3-d_1c_2\cos^2(q_1-q_2))^2} + \frac{d_1c_3u_1\sin(q_1-q_2)}{(c_3-d_1c_2\cos^2(q_1-q_2))^2} + \frac{d_1^2c_2u_1\sin(q_1-q_2)\cos^2(q_1-q_2)}{(c_3-d_1c_2\cos^2(q_1-q_2))^2}$$

$$+\frac{d_2c_2c_3\cos(q_1)-d_1d_2c_2^2\cos(q_1)\cos^2(q_1-q_2)}{(c_3-d_1c_2\cos^2(q_1-q_2))^2} - \frac{2d_1d_2c_2^2\sin(q_1)\sin(q_1-q_2)\cos(q_1-q_2)}{(c_3-d_1c_2\cos^2(q_1-q_2))^2}$$

$$+\frac{c_2c_3\dot{q}_1^2\cos(q_1-q_2)-d_1c_2^2\dot{q}_1^2\cos^3(q_1-q_2)}{(c_3-d_1c_2\cos^2(q_1-q_2))^2} - \frac{2d_1c_2^2\dot{q}_1^2\sin^2(q_1-q_2)\cos(q_1-q_2)}{(c_3-d_1c_2\cos^2(q_1-q_2))^2}$$

$$+\frac{2d_1c_2c_3\sin(q_2)\sin(q_1-q_2)\cos(q_1-q_2)}{(c_3-d_1c_2\cos^2(q_1-q_2))^2} + \frac{d_1c_2c_3\dot{q}_2^2\cos^2(q_1-q_2)-d_1^2c_2^2\dot{q}_2^2\cos^4(q_1-q_2)}{(c_3-d_1c_2\cos^2(q_1-q_2))^2}$$

$$-\frac{d_1c_2c_3\dot{q}_2^2\sin^2(q_1-q_2)}{(c_3-d_1c_2\cos^2(q_1-q_2))^2} - \frac{d_1^2c_2^2\dot{q}_2^2\sin^2(q_1-q_2)\cos^2(q_1-q_2)}{(c_3-d_1c_2\cos^2(q_1-q_2))^2},$$

$$\frac{\partial f_2}{\partial q_2} = \frac{2d_1c_2u_2\sin(q_1-q_2)\cos(q_1-q_2)}{(c_3-d_1c_2\cos^2(q_1-q_2))^2} - \frac{d_1c_3u_1\sin(q_1-q_2)}{(c_3-d_1c_2\cos^2(q_1-q_2))^2} - \frac{d_1^2c_2u_1\sin(q_1-q_2)\cos^2(q_1-q_2)}{(c_3-d_1c_2\cos^2(q_1-q_2))^2}$$

$$+\frac{2d_1d_2c_2^2\sin(q_1)\sin(q_1-q_2)\cos(q_1-q_2)}{(c_3-d_1c_2\cos^2(q_1-q_2))^2} - \frac{c_2c_3\dot{q}_1^2\cos(q_1-q_2)+d_1c_2^2\cos^3(q_1-q_2)}{(c_3-d_1c_2\cos^2(q_1-q_2))^2} + \frac{2d_1c_2^2\dot{q}_1^2\sin^2(q_1-q_2)\cos(q_1-q_2)}{(c_3-d_1c_2\cos^2(q_1-q_2))^2}$$

$$-\frac{c_3c_5\cos(q_2)+d_1c_2c_5\cos(q_2)\cos^2(q_1-q_2)}{(c_3-d_1c_2\cos^2(q_1-q_2))^2} - \frac{2d_1c_2c_5\sin(q_2)\sin(q_1-q_2)\cos(q_1-q_2)}{(c_3-d_1c_2\cos^2(q_1-q_2))^2}$$

$$-\frac{d_1c_2c_3\dot{q}_2^2\cos^2(q_1-q_2)+d_1^2c_2^2\dot{q}_2^2\cos^4(q_1-q_2)}{(c_3-d_1c_2\cos^2(q_1-q_2))^2} + \frac{d_1c_2c_3\dot{q}_2^2\sin^2(q_1-q_2)}{(c_3-d_1c_2\cos^2(q_1-q_2))^2}$$

$$+\frac{d_1^2c_2^2\dot{q}_2^2\sin^2(q_1-q_2)\cos^2(q_1-q_2)}{(c_3-d_1c_2\cos^2(q_1-q_2))^2},$$

$$\frac{\partial f_2}{\partial \dot{q}_1} = \frac{2c_2\dot{q}_1\sin(q_1-q_2)}{c_3-d_1c_2\cos^2(q_1-q_2)},$$

$$\frac{\partial f_2}{\partial \dot{q}_2} = \frac{2d_1c_2\dot{q}_2\sin(q_1-q_2)\cos(q_1-q_2)}{c_3-d_1c_2\cos^2(q_1-q_2)},$$

$$\frac{\partial f_2}{\partial u_1} = \frac{-d_1\cos(q_1-q_2)}{c_3-d_1c_2\cos^2(q_1-q_2)},$$

$$\frac{\partial f_2}{\partial u_2} = \frac{1}{c_3-d_1c_2\cos^2(q_1-q_2)}.$$

The elements of **A**, **B**, **C** and **D** matrices for Model 2.

$$\ddot{q}_1(q,\dot{q},u) = f_1(q,\dot{q},u) = \frac{u_1}{c_1} - \frac{d_1\cos(q_1-q_2)u_2}{c_3-d_1c_2\cos^2(q_1-q_2)} + \frac{d_1^2\cos^2(q_1-q_2)u_1}{c_3-d_1c_2\cos^2(q_1-q_2)}$$

$$-\frac{d_1^2c_2\cos^2(q_1-q_2)\sin(q_1-q_2)\dot{q}_2^2}{c_3-d_1c_2\cos^2(q_1-q_2)} - \frac{d_1c_2\cos(q_1-q_2)\sin(q_1-q_2)\dot{q}_1^2}{c_3-d_1c_2\cos^2(q_1-q_2)} - d_1\sin(q_1-q_2)\dot{q}_2^2,$$

$$\ddot{q}_2(q,\dot{q},u) = f_2(q,\dot{q},u) = \frac{u_2}{c_3-d_1c_2\cos^2(q_1-q_2)} - \frac{d_1\cos(q_1-q_2)u_1}{c_3-d_1c_2\cos^2(q_1-q_2)}$$

$$+\frac{d_1c_2\cos(q_1-q_2)\sin(q_1-q_2)\dot{q}_2^2}{c_3-d_1c_2\cos^2(q_1-q_2)} + \frac{c_2\sin(q_1-q_2)\dot{q}_1^2}{c_3-d_1c_2\cos^2(q_1-q_2)},$$

$$\frac{\partial f_1}{\partial q_1} = \frac{d_1 c_3 u_2 \sin(q_1-q_2)}{(c_3 - d_1 c_2 \cos^2(q_1-q_2))^2} + \frac{d_1^2 c_2 u_2 \sin(q_1-q_2)\cos^2(q_1-q_2)}{(c_3 - d_1 c_2 \cos^2(q_1-q_2))^2} - \frac{2d_1^2 c_3 u_1 \sin(q_1-q_2)\cos(q_1-q_2)}{(c_3 - d_1 c_2 \cos^2(q_1-q_2))^2}$$

$$- \frac{d_1 c_2 c_3 \dot{q}_1^2 \cos^4(q_1-q_2)}{(c_3 - d_1 c_2 \cos^2(q_1-q_2))^2} + \frac{d_1^2 c_2^2 \dot{q}_1^2 \cos^4(q_1-q_2)}{(c_3 - d_1 c_2 \cos^2(q_1-q_2))^2} + \frac{d_1 c_2 c_3 \dot{q}_1^2 \sin^2(q_1-q_2)}{(c_3 - d_1 c_2 \cos^2(q_1-q_2))^2}$$

$$+ \frac{d_1^2 c_2^2 \dot{q}_1^2 \sin^2(q_1-q_2)\cos^2(q_1-q_2)}{(c_3 - d_1 c_2 \cos^2(q_1-q_2))^2} - \frac{d_1^2 c_2 c_3 \dot{q}_2^2 \cos^3(q_1-q_2)}{(c_3 - d_1 c_2 \cos^2(q_1-q_2))^2} + \frac{d_1^3 c_2^2 \dot{q}_2^2 \cos^5(q_1-q_2)}{(c_3 - d_1 c_2 \cos^2(q_1-q_2))^2}$$

$$+ \frac{2d_1^2 c_2 c_3 \dot{q}_2^2 \sin^2(q_1-q_2)\cos(q_1-q_2)}{(c_3 - d_1 c_2 \cos^2(q_1-q_2))^2} - d_1 \dot{q}_2^2 \cos(q_1-q_2),$$

$$\frac{\partial f_2}{\partial \dot{q}_2} = \frac{2d_1 c_2 \dot{q}_2 \sin(q_1-q_2)\cos(q_1-q_2)}{c_3 - d_1 c_2 \cos^2(q_1-q_2)},$$

$$\frac{\partial f_2}{\partial u_1} = \frac{-d_1 \cos(q_1-q_2)}{c_3 - d_1 c_2 \cos^2(q_1-q_2)},$$

$$\frac{\partial f_1}{\partial q_2} = \frac{-d_1 u_2 c_3 \sin(q_1-q_2)}{(c_3 - d_1 c_2 \cos^2(q_1-q_2))^2} - \frac{d_1^2 c_2 u_2 \sin(q_1-q_2)\cos^2(q_1-q_2)}{(c_3 - d_1 c_2 \cos^2(q_1-q_2))^2} - \frac{2d_1^2 c_2 c_3 u_1 \sin(q_1-q_2)\cos(q_1-q_2)}{(c_3 - d_1 c_2 \cos^2(q_1-q_2))^2}$$

$$+ \frac{4d_1^3 c_2 u_1 \sin(q_1-q_2)\cos^3(q_1-q_2)}{(c_3 - d_1 c_2 \cos^2(q_1-q_2))^2} + \frac{d_1 c_2 c_3 \dot{q}_1^2 \cos^2(q_1-q_2)}{(c_3 - d_1 c_2 \cos^2(q_1-q_2))^2} - \frac{d_1^2 c_2^2 \dot{q}_1^2 \cos^4(q_1-q_2)}{(c_3 - d_1 c_2 \cos^2(q_1-q_2))^2}$$

$$- \frac{d_1 c_2 c_3 \dot{q}_1^2 \sin^2(q_1-q_2)}{(c_3 - d_1 c_2 \cos^2(q_1-q_2))^2} - \frac{d_1^2 c_2^2 \dot{q}_1^2 \sin^2(q_1-q_2)\cos^2(q_1-q_2)}{(c_3 - d_1 c_2 \cos^2(q_1-q_2))^2} + \frac{d_1^2 c_2 c_3 \dot{q}_2^2 \cos^3(q_1-q_2)}{(c_3 - d_1 c_2 \cos^2(q_1-q_2))^2}$$

$$- \frac{d_1^3 c_2^2 \dot{q}_2^2 \cos^5(q_1-q_2)}{(c_3 - d_1 c_2 \cos^2(q_1-q_2))^2} - \frac{2d_1^2 c_2 c_3 \dot{q}_2^2 \sin^2(q_1-q_2)\cos(q_1-q_2)}{(c_3 - d_1 c_2 \cos^2(q_1-q_2))^2} + d_1 \dot{q}_2^2 \cos(q_1-q_2),$$

$$\frac{\partial f_1}{\partial \dot{q}_1} = \frac{-2d_1 c_2 \dot{q}_1 \sin(q_1-q_2)\cos(q_1-q_2)}{c_3 - d_1 c_2 \cos^2(q_1-q_2)},$$

$$\frac{\partial f_1}{\partial \dot{q}_2} = \frac{-2d_1^2 c_2 \dot{q}_2 \sin(q_1-q_2)\cos^2(q_1-q_2)}{c_3 - d_1 c_2 \cos^2(q_1-q_2)} - 2d_1 \dot{q}_2 \sin(q_1-q_2),$$

$$\frac{\partial f_1}{\partial u_1} = \frac{1}{c_1} + \frac{d_1^2 \cos^2(q_1-q_2)}{c_3 - d_1 c_2 \cos^2(q_1-q_2)},$$

$$\frac{\partial f_1}{\partial u_2} = \frac{-d_1 \cos(q_1-q_2)}{c_3 - d_1 c_2 \cos^2(q_1-q_2)},$$

$$\frac{\partial f_2}{\partial q_1} = -\frac{2d_1 c_2 \sin(q_1-q_2)\cos(q_1-q_2)}{(c_3 - d_1 c_2 \cos^2(q_1-q_2))^2} + \frac{d_1 c_3 u_1 \sin(q_1-q_2)}{(c_3 - d_1 c_2 \cos^2(q_1-q_2))^2} + \frac{d_1^2 c_2 u_1 \sin(q_1-q_2)\cos(q_1-q_2)}{(c_3 - d_1 c_2 \cos^2(q_1-q_2))^2}$$

$$+ \frac{c_2 c_3 \dot{q}_1^2 \cos(q_1-q_2) - d_1 c_2^2 \dot{q}_1^2 \cos^3(q_1-q_2)}{(c_3 - d_1 c_2 \cos^2(q_1-q_2))^2} - \frac{2d_1 c_2^2 \dot{q}_1^2 \sin^2(q_1-q_2)\cos(q_1-q_2)}{(c_3 - d_1 c_2 \cos^2(q_1-q_2))^2}$$

$$+ \frac{d_1 c_2 c_3 \dot{q}_2^2 \cos^2(q_1-q_2) - d_1^2 c_2^2 \dot{q}_2^2 \cos^4(q_1-q_2)}{(c_3 - d_1 c_2 \cos^2(q_1-q_2))^2} - \frac{d_1 c_2 c_3 \dot{q}_2^2 \sin^2(q_1-q_2)}{(c_3 - d_1 c_2 \cos^2(q_1-q_2))^2} -$$

$$- \frac{d_1^2 c_2^2 \dot{q}_2^2 \sin^2(q_1-q_2)\cos^2(q_1-q_2)}{(c_3 - d_1 c_2 \cos^2(q_1-q_2))^2},$$

$$\frac{\partial f_2}{\partial q_2} = \frac{2d_1c_2u_2\sin(q_1-q_2)\cos(q_1-q_2)}{(c_3-d_1c_2\cos^2(q_1-q_2))^2} - \frac{d_1c_3u_1\sin(q_1-q_2)}{(c_3-d_1c_2\cos^2(q_1-q_2))^2} - \frac{d_1^2c_2u_1\sin(q_1-q_2)\cos^2(q_1-q_2)}{(c_3-d_1c_2\cos^2(q_1-q_2))^2}$$

$$-\frac{c_2c_3\dot{q}_1^2\cos(q_1-q_2)+d_1c_2^2\cos^3(q_1-q_2)}{(c_3-d_1c_2\cos^2(q_1-q_2))^2} + \frac{2d_1c_2^2\dot{q}_1^2\sin^2(q_1-q_2)\cos(q_1-q_2)}{(c_3-d_1c_2\cos^2(q_1-q_2))^2}$$

$$-\frac{d_1c_2c_3\dot{q}_2^2\cos^2(q_1-q_2)+d_1^2c_2^2\dot{q}_2^2\cos^4(q_1-q_2)}{(c_3-d_1c_2\cos^2(q_1-q_2))^2} + \frac{d_1c_2c_3\dot{q}_2^2\sin^2(q_1-q_2)}{(c_3-d_1c_2\cos^2(q_1-q_2))^2} + \frac{d_1^2c_2^2\dot{q}_2^2\sin^2(q_1-q_2)\cos^2(q_1-q_2)}{(c_3-d_1c_2\cos^2(q_1-q_2))^2},$$

$$\frac{\partial f_2}{\partial \dot{q}_1} = \frac{2c_2\dot{q}_1\sin(q_1-q_2)}{c_3-d_1c_2\cos^2(q_1-q_2)},$$

$$\frac{\partial f_2}{\partial u_2} = \frac{1}{c_3-d_1c_2\cos^2(q_1-q_2)}.$$

Acknowledgements. This work has been supported by the Applied Research Programme of the National Centre for Research and Development as a project ID 178438 path A – Costume for acquisition of human movement based on IMU sensors with collection, visualization and data analysis software.

R EFERENCES

[1] M. Lazarević, "Mechanics of human locomotor system", *FME Transactions* 34 (2), 105–114 (2006).

[2] D. Lee, M. Glueck, A. Khan, E. Fiume, and K. Jackson, "A survey of modeling and simulation of skeletal muscle", *ACM Trans. on Graphics* 28 (4), (2010).

[3] J.K. Lee and E.J. Park, "A fast quaternion-based orientation optimizer via virtual rotation for human motion tracking", *IEEE Trans. on Biomedical Engineering* 56 (5), 1574–1582 (2009).

[4] H. van der Kooij, B. Koopman, and F.C.T. van der Helm, "Human motion control", *Reader for Delft University course wb2407 and Twente University course* 115047, 211–220 (2008).

[5] Z.Q. Zhang, W.C. Wong, and J.K. Wu, "Ubiquitous human upper-limb motion estimation using Wearable sensors", *IEEE Trans. on Information Technology in Biomedicine* 15 (4), 513–521 (2011).

[6] E. Burdet, K.P. Tee, I. Mareels, T.E. Milner, C.M. Chew, D.W. Franklin, R. Osu, and M. Kawato, "Stability and motor adaptation in human arm movements", *Biological Cybernetics* 94 (1), 20–32 (2006).

[7] A. Kadiallah, D.W. Franklin, and E. Burdet, "Generalization in adaptation to stable and unstable dynamics", *PLoS ONE* 7 (10), CD-ROM (2012).

[8] M.J. Fu and M.C. Cavusoglu, "Human-arm-and-hand-dynamic model with variability analyses for a stylus-based haptic interface", *IEEE Trans. on Systems, Man, and Cybernetics, Part B: Cybernetics* 42 (6), 1633–1644 (2012).

[9] W. Li, "Optimal control for biological movement systems", *Ph.D. Thesis*, University of California, San Diego, 2006.

[10] D. Liu and E. Todorov, "Hierarchical optimal control of a 7-DOF arm model", *IEEE Symp. on Adaptive Dynamic Programming and Reinforcement Learning* 1, 50–57 (2009).

[11] P.R. Culmer, A.E. Jackson, S. Makower, R. Richardson, J.A. Cozens, M.C. Levesley, and B.B. Bhakta, "A control strategy for upper limb robotic rehabilitation with a dual robot system", *IEEE/ASME Tran. on Mechatronics* 15 (4), 575–585 (2010).

[12] P.K. Artemiadis and K.J. Kyriakopoulos, "EMG-based control of a robot arm using low-dimensional embeddings", *IEEE Trans. on Robotics* 26 (2), 393–398 (2010).

[13] P.K. Artemiadis and K.J. Kyriakopoulos, "A switching regime model for the EMG-based control of a robot arm", *IEEE Trans. on Systems, Man, and Cybernetics, Part B: Cybernetics* 41 (1), 53–63 (2011).

[14] F.I. Sheikh, "Real-time human arm motion translation for the WorkPartner robot", *Master Thesis*, Luleå University of Technology, Kiruna, 2008.

[15] G. Angelosanto, "Kalman filtering of IMU sensor for robot balance control", *Bachelor Thesis*, Massachusetts Institute of Technology, Cambridge, 2008.

[16] M. El-Gohary and J. McNames, "Shoulder and elbow joint angle tracking with inertial sensors", *IEEE Trans. on Biomedical Engineering* 59 (9), 2635–2641 (2012).

[17] H. Fourati, N. Manamanni, L. Afilal, and Y. Handrich, "Complementary observer for body segments motion capturing by inertial and magnetic sensors", *IEEE/ASME Trans. on Mechatronics* 1, 1–9 (2012).

[18] S.H. Lee, "Biomechanical modeling and control of the human body for computer animation", *Ph.D. Thesis*, University of California, Los Angeles, 2008.

[19] Y.S. Suh, "Orientation estimation using a quaternion-based indirect Kalman filter with adaptive estimation of external acceleration", *IEEE Trans. on Instrumentation and Measurement* 59 (12), 3296–3305 (2010).

[20] A. Rodriguez-Angeles, A. Morales-Diaz, J.C. Bernabeě, and G. Arechavaleta, "An online inertial sensor-guided motion control for tracking human arm movements by robots", *Proc. 3rd IEEE RAS and EMBS Int. Conf. on Biomedical Robotics and Biomechatronics (BioRob)* 1, 319–324 (2010).

[21] A. Wang and M. Deng, "Human arm-like robot control using the viscoelasticity of human multi-joint arm", *Proc. 5th Int. Conf. on Computer Sciences and Convergence Information Technology (ICCIT)* 1, 738–743 (2010).

[22] J. Yu, J. Zhong-Ping, and Q. Ning, "Optimal control mechanisms in human arm reaching movements", *Proc. 30th Chinese Control Conference (CCC)* 1, 1377–1382 (2011).

[23] P.H. Chang, K. Park, S. Hoon Kang, H.I. Krebs, and N. Hogan, "Stochastic estimation of human arm impedance using robots with nonlinear frictions: an experimental validation", *IEEE/ASME Transactions on Mechatronics* 18 (2), 775–786 (2013).

[24] H. Moon, N. Hoang, N.P. Robson, and R. Langari, "Human arm motion planning against a joint constraint", *Proc. 4th IEEE RAS & EMBS Int. Conf. on Biomedical Robotics and Biomechatronics (BioRob)* 1, 401–406 (2012).

[25] N. Klopčar and J. Lenarčič, "Kinematic model for determination of human arm reachable workspace", *Meccanica* 40 (2), 203–219 (2005).

[26] W. Gallagher, M. Ding, and J. Ueda, "Relaxed individual control of skeletal muscle forces via physical human-robot interaction", *Multibody System Dynamics* 30 (1), 77–99 (2013).

[27] P.K. Artemiadis, P.T. Katsiaris, and K.J. Kyriakopoulos, "A biomimetic approach to inverse kinematics for a redundant robot arm", *Autonomous Robots* 29 (3–4), 293–308 (2010).

[28] R.R. Porle, A. Chekima, F. Wong, and G. Sainarayanan, "Multiple features integration in 2D upper human body pose modelling system", *Proc. 10th Int. Conf. on Information Sciences Signal Processing and their Applications (ISSPA)* 1, 570–573 (2010).

[29] Y.R. Chen, C.M. Huang, and L.C. Fu, "Visual tracking of human head and arms with a single camera", *Proc. IEEE/RSJ Int. Conf. on Intelligent Robots and Systems (IROS)* 1, 3416–3421 (2010).

[30] T. Kashima, K. Yanagihara, and M. Iwaseya, "Trajectory formation based on a human arm model with redundancy", *Proc. IEEE Int. Conf. on Systems, Man, and Cybernetics (SMC)* 1, 959–963 (2012).

[31] S. Djebrani, A. Benali, and F. Abdessemed, "Modelling and control of an omnidirectional mobile manipulator", *Int. J. Applied Mathematics and Computer Science* 22 (3), 601–616 (2012).

[32] T. Kaczorek, A. Dzieliński, W. Dąbrowski, and R. Łopatka, *Principles of Control Theory*, WNT, Warszawa, 2009, (in Polish).

[33] G.G. Rigatos, "A derivative-free Kalman filtering approach to state estimation-based control of nonlinear systems, *IEEE Trans. on Industrial Electronics* 59 (10), 3987–3997 (2012).

[34] D. Simon, "Kalman filtering with state constraints: a survey of linear and nonlinear algorithms", *Control Theory & Applications* 4 (8), 1303–1318 (2010).

[35] C.M. Kwan and F.L. Lewis, "A note on Kalman filtering", *IEEE Trans. on Education* 42 (3), 225–227 (1999).

[36] B. Teixeira, J. Chandrasekar, H.J. Palanthandalam-Madapusi, L. Torres, L.A. Aguirre, and D.S. Bernstein, "Gain-constrained Kalman filtering for linear and nonlinear systems", *IEEE Trans. on Signal Processing* 56 (9), 4113–4123 (2008).

[37] J. Korbicz, M. Witczak, and V. Puig, "LMI-based strategies for designing observers and unknown input observers for nonlinear discrete-time systems", *Bull. Pol. Ac.: Tech.* 55 (1), 31–42 (2007).

[38] K. Szabat, T. Orłowska-Kowalska, and K.P. Dyrcz, "Extended Kalman filters in the control structure of two-mass drive system", *Bull. Pol. Ac.: Tech.* 54 (3), 315–325 (2006).

[39] T. Orłowska-Kowalska, M. Kamiński, and K. Szabat, "Mechanical state variable estimation of drive system with elastic coupling using optimised feed-forward neural networks", *Bull. Pol. Ac.: Tech.* 56 (3), 239–246 (2008).

[40] Z. Chen, "Bayesian filtering: from Kalman filters to particle filters, and beyond", *Statistics* 182 (1), 1–69 (2003).

[41] S. Saha and F. Gustafsson, "Particle filtering with dependent noise processes", *IEEE Trans. on Signal Processing* 60 (9), 4497–4508 (2012).

[42] H.A.P. Blom and E.A. Bloem, "Exact Bayesian and particle filtering of stochastic hybrid systems", *IEEE Trans.s on Aerospace and Electronic Systems* 43 (1), 55–70 (2007).

[43] P.M. Djuric, J.H. Kotecha, J. Zhang, Y. Huang, T. Ghirmai, M.F. Bugallo, and J. Miguez, "Particle filtering", *IEEE Signal Processing Magazine* 20 (5), 19–38 (2003).

[44] D. Yee, J.P. Reilly, T. Kirubarajan, and K. Punithakumar, "Approximate conditional mean particle filtering for linear/nonlinear dynamic state space models", *IEEE Trans. on Signal Processing* 56 (12), 5790–5803 (2008).

[45] M.S. Arulampalam, S. Maskell, N. Gordon, and T. Clapp, "A tutorial on particle filters for online nonlinear/non-Gaussian Bayesian tracking", *IEEE Trans. on Signal Processing* 50 (2), 174–188 (2002).

[46] K. Jaskot and A. Babiarz, "The inertial measurement unit for detection of position", *Electrical Engineering Review* 86 (11a), 323–333 (2010).